DR-0097-3

T-14875

ORNL/FEDC-83/10

EQUILIBRIUM MODELING OF THE TFCX POLOIDAL FIELD COIL SYSTEM

D.J. STRICKLER
J.B. MILLER
K.E. ROTHE
Y-K.M. PENG

ORNL/FEDC--83/10

DE84 012040

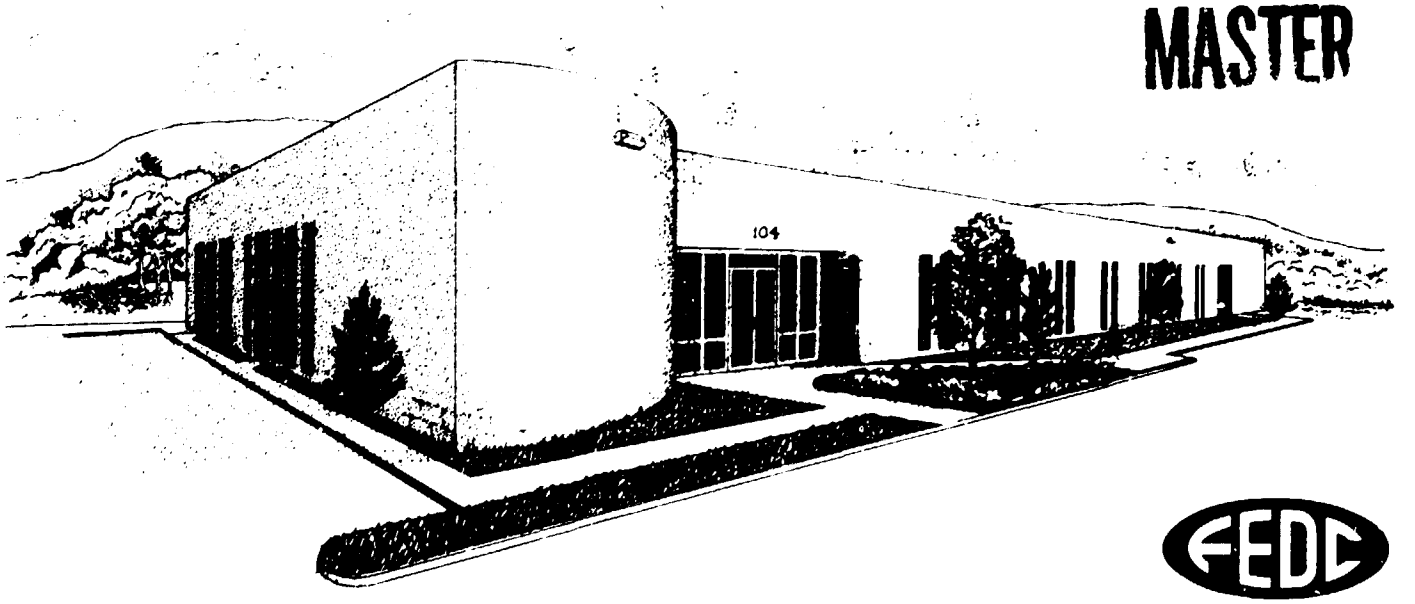

FEDC

FUSION ENGINEERING DESIGN CENTER

Oak Ridge National Laboratory • Oak Ridge, Tennessee

ORNL/FEDC-83/10
Dist. Category UC-20 c,d

Fusion Energy Division

EQUILIBRIUM MODELING OF THE TFCX POLOIDAL FIELD COIL SYSTEM

D. J. Strickler
J. B. Miller
K. E. Rothe
Y-K. M. Peng

Date Published - April 1984

NOTICE This document contains information of a preliminary nature. It is subject to revision or correction and therefore does not represent a final report.

Prepared by the
OAK RIDGE NATIONAL LABORATORY
Oak Ridge, Tennessee 37831
operated by
UNION CARBIDE CORPORATION
for the
U.S. DEPARTMENT OF ENERGY
under Contract No. W-7405-eng-26

CONTENTS

LIST OF FIGURES v

LIST OF TABLES vii

ABSTRACT ix

1. INTRODUCTION 1

2. METHOD OF ANALYSIS 3

2.1 The Poloidal Field Coil Design Process 3

2.2 The FEDC MHD Equilibrium Code 5

2.3 Plasma Flux Requirements 12

2.4 Plasma Scrapeoff Considerations 13

3. POLOIDAL COIL DESIGN OPTIONS FOR THE TFCX 15

3.1 Impact on System Trade Studies 15

3.2 TFCX-S 17

3.3 TFCX-H 22

4. POLOIDAL COIL CURRENT SCENARIOS FOR THE TFCX 22

4.1 Plasma Startup 22

4.2 Plasma Heating 28

4.3 Quasi-Steady-State Operation 37

5. SUMMARY AND CONCLUSIONS 37

REFERENCES 41

LIST OF FIGURES

1	Elevation view of the TFCX-S poloidal field coil system showing the coil numbering scheme	2
2	The PF coil design process applied in the preconceptual design analysis of the TFCX	6
3	Dependence of the relative error (ε) in flux values at the prescribed plasma boundary ∂P, total coil current, and triangularity on increasing α (Eq. 5)	9
4	Contours of constant axis and limiter values of q (q_o = 1.0, q_L = 2.0) in the profile parameters A and B (Eq. 6) for plasma parameters in the range of TFCX options (R_o = 3.6 m, a = 0.75 m, κ = 1.6, δ = 0.3, and B_t = 7.0 T). Current profiles (insert) vary along these contours	11
5	Some fraction of the field lines in the scrapeoff region may be diverted outside the plasma chamber in highly elongated and D-shaped plasmas	14
6	For plasma cross sections of the same elongation (κ = 1.60) and triangularity (δ = 0.38), the sensitivity of the shape of field lines in the plasma scrapeoff region to different boundary shape paramaterizations is shown using (a) Eq. (13) and (b) Eq. (14)	16
7	High beta ($\langle\beta\rangle$ = 6.1%) TFCX-S equilibrium poloidal flux surfaces for a fully discharged OH solenoid (I_{OH} = -28 MA) at the end of burn t = t_F	21
8	The TFCX-H poloidal field coil system	26
9	High beta ($\langle\beta\rangle$ = 5.3%) TFCX-H equilibrium poloidal flux surfaces for a fully discharged OH solenoid (I_{OH} = -30 MA) at the end of burn t = t_F	27
10	TFCX-S: (a) plasma, OH current, volt-seconds and (b) poloidal coil current waveforms for totally rf startup	33
11	TFCX-H: (a) plasma, OH current, volt-seconds and (b) poloidal coil current waveforms for totally rf startup	33
12	TFCX-S: (a) plasma, OH current, and volt-seconds waveforms for rf-assisted startup and (b) poloidal coil currents	36
13	TFCX-S: (a) OH solenoid current (I_{OH}), plasma current (I_p), and volt-second (Φ) waveforms and (b) OH solenoid current (I_{OH}), shaping field current (I_{SF}), and outboard equilibrium field coil current (I_{EF}) for quasi-steady-state operation	38

LIST OF TABLES

1	TFCX-S data from systems code	18
2	TFCX-S coil locations and currents	19
3	TFCX-S plasma parameters	20
4	TFCX-H data from systems code	23
5	TFCX-H coil locations and currents	24
6	TFCX-H plasma parameters	25
7	TFCX-S coil currents for totally rf startup	29
8	TFCX-S plasma parameters for totally rf startup	30
9	TFCX-H coil currents for totally rf startup	31
10	TFCX-H plasma parameters for totally rf startup	32
11	TFCX-S coil currents for rf-assisted startup	34
12	TFCX-S plasma parameters for rf-assisted startup	35

1. INTRODUCTION

The Toroidal Fusion Core Experiment (TFCX) is proposed to be a tokamak ignition device with a low safety factor ($q = 2.0$), rf or rf-assisted startup, long inductive burn pulse ($\sim$300 s), and an elongated plasma cross section ($\kappa = 1.6$) with moderate triangularity ($\delta = 0.3$). Design options include all-superconducting toroidal field (TF) coils (TFCX-S) or possibly a hybrid TF coil system with copper insert coils (TFCX-H) to increase the field on-axis. The current-drive assumption implies the possibility of quasi-steady-state operation through the periodic recharging of an ohmic heating (OH) solenoid. System trade studies are in progress to assist in choosing an appropriate candidate for the TFCX conceptual design. Reference design points for the all superconducting and hybrid options have been chosen. In this work, an analysis is presented of the poloidal field (PF) configurations, coil locations, and coil current waveforms consistent with the magnetohydrodynamic (MHD) equilibrium and plasma volt-second requirements for the reference TFCX options of this trade study. Major plasma and machine parameters for the TFCX are the result of a systems analysis [1], which includes the PF system analysis as an important element.

Given the plasma geometry and a set of performance parameters [e.g., maximum stable beta $\beta_{max} = 0.117a(1 + \kappa^2)/R_o q$] from a Fusion Engineering Design Center (FEDC) tokamak systems code [2] simulation with an assumed constant ignition margin (I_g) of 1.0, the purpose of this analysis is to determine a PF coil system that satisfies (1) volt-second requirements, (2) mechanical configuration constraints, (3) maximum field constraints at the superconducting PF coils, and (4) plasma shape requirements for each TF coil option. The methods of analysis are discussed in Sect. 2.

In this analysis, a PF system consists of three coil groups (Fig. 1)—an OH central solenoid, shaping field (SF) coils, and outboard equilibrium field (EF) coils. PF coils are assumed to be superconducting and are positioned external to the TF coils and associated structures. Coil locations are also constrained by maintenance and machine access

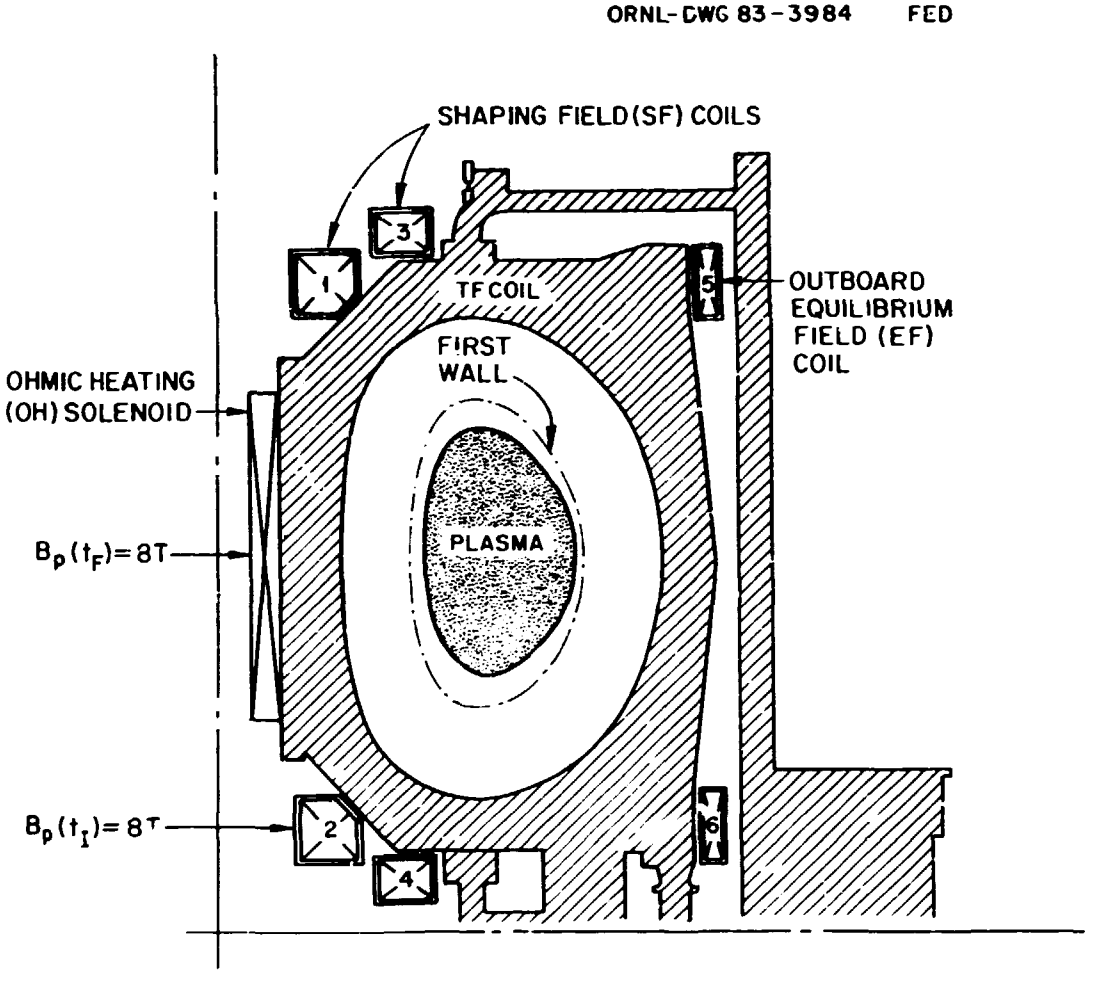

Fig. 1. Elevation view of the TFCX-S poloidal field coil system showing the coil numbering scheme.

considerations. The fields of the three sets of coils are coupled — a concept that reduces the total ampere-turns and allows the magnetic energy stored in the system to be used for both plasma current buildup and MHD equilibrium. The coupled-coil concept may, however, present additional plasma control problems not addressed in this study. PF coil systems for the reference cases (TFCX-S and TFCX-H) are presented in Sect. 3.

Poloidal coil current waveforms for the TFCX consistent with the plasma startup, heating, and burn phases are discussed in Sect. 4. The prospect of current drive at relatively low density also leads to a possible scenario for quasi-steady-state operation in which, following a current initiation and ramp phase, the OH solenoid is alternately (1) discharged during a 150- to 200-s, high-beta, inductive burn cycle and (2) recharged during a approximate 30-s rf current-drive cycle at low beta. PF coil currents consistent with this mode of operation also need to satisfy the flux requirements of a plasma cool-down period prior to solenoid recharge, and one such possible set of waveforms is presented.

2. METHOD OF ANALYSIS

2.1 THE POLOIDAL FIELD COIL DESIGN PROCESS

The design configuration for a given TFCX option is the result of an iterative process involving the use of the FEDC MHD equilibrium code, the EFFI [3] magnetics code, and the FEDC tokamak systems code. The systems code is used to establish an operating point (i.e., parameters such as the plasma major radius R_o, minor radius a, vacuum toroidal field B_t, and maximum volume-averaged beta $<\beta>$) consistent with the TFCX assumptions of q = 2.0, an ignition margin (I_g) of 1.0, and a radial build that satisfies volumetric heating requirements and TF ripple constraints. These data lead to a mechanical configuration that defines a set of possible regions in which to locate PF coils. The FEDC equilibrium code and the EFFI code are used to actually locate these coils and to determine if the system is feasible with respect to volt-second, maximum field, and plasma shape requirements.

The first step in defining PF coil locations is to compute the maximum radial position and size of the OH solenoid. These are determined by magnetic field and MHD equilibrium calculations for an assumed solenoid current density, typically $J_{OH} = 1.5 \times 10^7$ A/m^2. For a totally discharged solenoid at the end of the plasma burn phase ($t = t_F$), the maximum poloidal magnetic field at a PF coil occurs near the midplane on the inboard side of the solenoid and is modeled by computing the field of the OH and outboard EF coils only. This is a conservative estimate because the plasma and SF coil currents run in a different direction and because including these fields would tend to reduce the total field. The maximum solenoid mean radius and width are determined by the condition $B_p^{max} \lesssim 8$ T (i.e., the maximum allowable field at a superconducting PF coil) and by configurational constraints set by the TF coil structure and bucking cylinder. Typically, one MHD equilibrium is necessary to approximate the outboard EF coil currents for use in this end of the burn field calculation.

For an assumed solenoid current (I_{OH}) at the initiation of the plasma burn $t = t_I$, the SF coil locations are adjusted in a series of MHD equilibrium calculations in order to achieve the desired plasma shape (i.e., an elongation satisfying $|\kappa - \kappa_o| < \varepsilon_\kappa$ and triangularity $|\delta - \delta_o| < \varepsilon_\delta$). The outboard EF coil locations are usually fixed by the machine design configuration. An iteration over the current $I_{OH}(t_I)$ is generally necessary to ensure that $B_p^{max} \lesssim 8$ T in the OH and SF coils at $t = t_I$. Here the OH, SF, and plasma currents usually run in the same direction, and all are included in the magnetic field calculation. The plasma is modeled in the EFFI calculation as having a rectangular cross section with an appropriate uniform current density. A final set of MHD equilibrium calculations is made at $t = t_F$, during which SF coil currents are found that approximate the prescribed plasma shape at the end of the inductive burn phase. Volt-seconds provided by the PF system during burn are computed from the equilibria at t_I and t_F to determine if the configuration and PF coil system are feasible with respect to plasma flux requirements.

If volt-seconds are inadequate, these iterations are nested inside an outermost loop involving systems code calculations at various R_o in

order to determine the minimum radius at which all PF system requirements are satisfied. The PF coil design procedure is summarized in Fig. 2.

2.2 THE FEDC MHD EQUILIBRIUM CODE

For a fixed OH solenoid current, estimates of SF and EF coil currents necessary to maintain a plasma of prescribed shape are obtained with the FEDC MHD equilibrium code solving the axisymmetric equilibrium equation in cylindrical (R,ϕ,Z) coordinates:

$$\Delta^*\psi \equiv R^2\nabla \cdot R^{-2}\nabla\psi = -\mu R J_\phi \ . \tag{1}$$

Here, J_ϕ is the toroidal plasma current density, and the poloidal flux function $\psi = \psi^P + \psi^e$ (where ψ^P is the flux due to the plasma current and ψ^e the flux due to external sources) satisfies

$$\psi^P(\vec{x}_b) = \iint_\Omega G(\vec{x}_b,\vec{x}) J_\phi(\vec{x}) d\Omega \tag{2}$$

for $\vec{x}_b = (R_b,Z_b)$ on the boundary of a rectangular region Ω. The Green's function G relates ψ at a point on the boundary to a unit current density at a point in Ω [4].

For fixed boundary values $\psi(\vec{x}_b) = \psi^P(\vec{x}_b) + \psi^e(\vec{x}_b)$ and current profile J_ϕ, the resulting elliptic partial differential equation [Eq. (1)] is discretized on a rectangular mesh (with typical dimensions 33 by 65 or 65 by 129), and the resulting linear equations are solved by a direct, cyclic reduction method using SEPX4 [5]. The iterative procedure

$$\Delta^*\psi^{(n+1)} = -\mu R \left[\alpha J_\phi^{(n+1)} + (1-\alpha) J_\phi^{(n)} \right] , \quad 0 < \alpha \leq 1 , \tag{3}$$

is used to solve for the current density

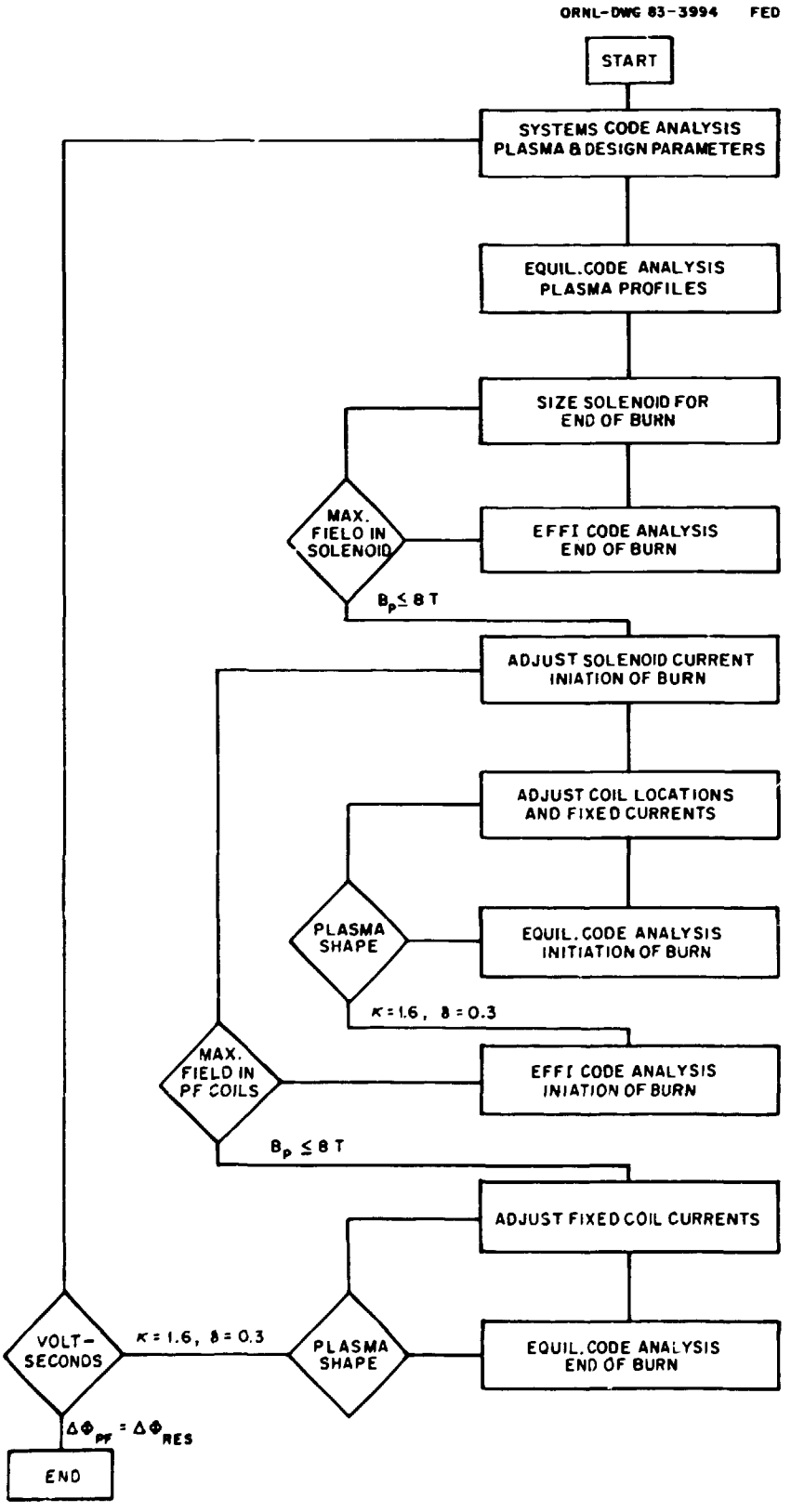

Fig. 2. The PF coil design process applied in the preconceptual design analysis of the TFCX.

$$J_\phi = R \frac{dP}{d\psi} + \frac{F}{\mu R} \frac{dF}{d\psi} \quad , \tag{4}$$

which depends nonlinearly on ψ through assumed plasma pressure $P(\psi)$ and toroidal magnetic flux, $F(\psi) = RB_t$, profiles. Prior to recomputing J_ϕ in this iteration, a correction in the external flux function ψ^e is made by adjusting some subset of the coil currents I_j so that the total flux at points on a prescribed plasma boundary, ∂P, is approximately constant. More specifically, if $\partial P = (R_i^p, Z_i^p)$ is a set of points describing a desired plasma shape and including a limiter point (R_L, Z_L), the approximation problem

$$\sum_i \left[\sum_j G(R_j, Z_j;\ R_i, Z_i) I_j - \psi^e(R_i, Z_i) \right]^2 + \alpha \sum_j I_j^2 = \text{minimum} \tag{5}$$

is solved for the variable coil currents I_j. Here the desired ψ^e is determined at the given plasma boundary points by $\psi^e(R_i, Z_i) = \psi_L - \psi^p(R_i, Z_i)$, where $\psi_L = \psi(R_L, Z_L)$ is the poloidal flux at a limiter point. Thus, the final coil currents I_i determined by the equilibrium code depend largely on coil locations (R_j, Z_j), $j = 1, 2, \ldots, N_c$; the plasma boundary points (R_i, Z_i), $i = 1, 2, \ldots, N_p$; and the regularization parameter α, which gives some weight to minimizing total ampere-turns. Some subset of the coil currents may be fixed during an equilibrium calculation, as is the case with the current loops representing the OH solenoid in the TFCX analysis.

Without the smoothing parameter α, coil currents often tend to oscillate in sign and vary widely in magnitude (compared to a practical solution). In practice, α is varied until the error in the flux values at the prescribed plasma boundary points

$$\varepsilon = \sum_i \left[\psi_i^e - \sum_j G_{ij} I_j \right]^2 \Big/ \sum_i \left[\psi_i^e \right]^2$$

meets a specified criterion or until some global plasma shaping parameters (e.g., κ and δ) are sufficiently close to the desired values. This

condition is demonstrated by Fig. 3, in which the dependence of ϵ and δ on changes in α are shown for a coil system consisting of 32 coils with centers equally spaced in arc length on a given curve in the poloidal plane.

The "limiter" value of the poloidal flux, ψ_L, is taken to be the minimum of the flux values at a prescribed point (R_L, Z_L) in the computational domain Ω and at a poloidal separatrix created by SF coils carrying current in the same direction as the plasma current. The latter situation occurs in modeling the equilibrium configuration of a poloidal divertor [6].

For the TFCX analysis, plasma pressure and toroidal magnetic flux profiles input to the FEDC equilibrium code through Eq. (4) are of the form:

$$\frac{dP}{dx} = P_o \left(\frac{e^{-Ax} - e^{-A}}{e^{-A} - 1} \right) ,$$

$$\frac{dF}{dx} = 2\pi R_o^2 P_o \left(\frac{1}{\beta_J} - 1 \right) \left(\frac{e^{-Bx} - e^{-B}}{e^{-B} - 1} \right) , \tag{6}$$

and

$$x = \frac{\psi - \psi_o}{\psi_L - \psi_o} ,$$

where ψ_o is the poloidal flux at the magnetic axis. Integrals of these profiles are chosen such that $P = 0$ and $F = R_o B_t$ at the plasma edge. During the iterative procedure described by Eq. (3), P_o is scaled by σ^2, where $\sigma = I_p / \iint J_\phi d\Omega$, to fix the plasma current I_p.

In the design process, the constants A and B in Eq. (6) are determined by calling the equilibrium code as a subroutine from the objective function used in the software package VMCON [7], a routine for numerical nonlinear optimization with constraints (possibly nonlinear). That is, the objective function $Q = (q_L/q_o - c)^2$ is minimized with respect to

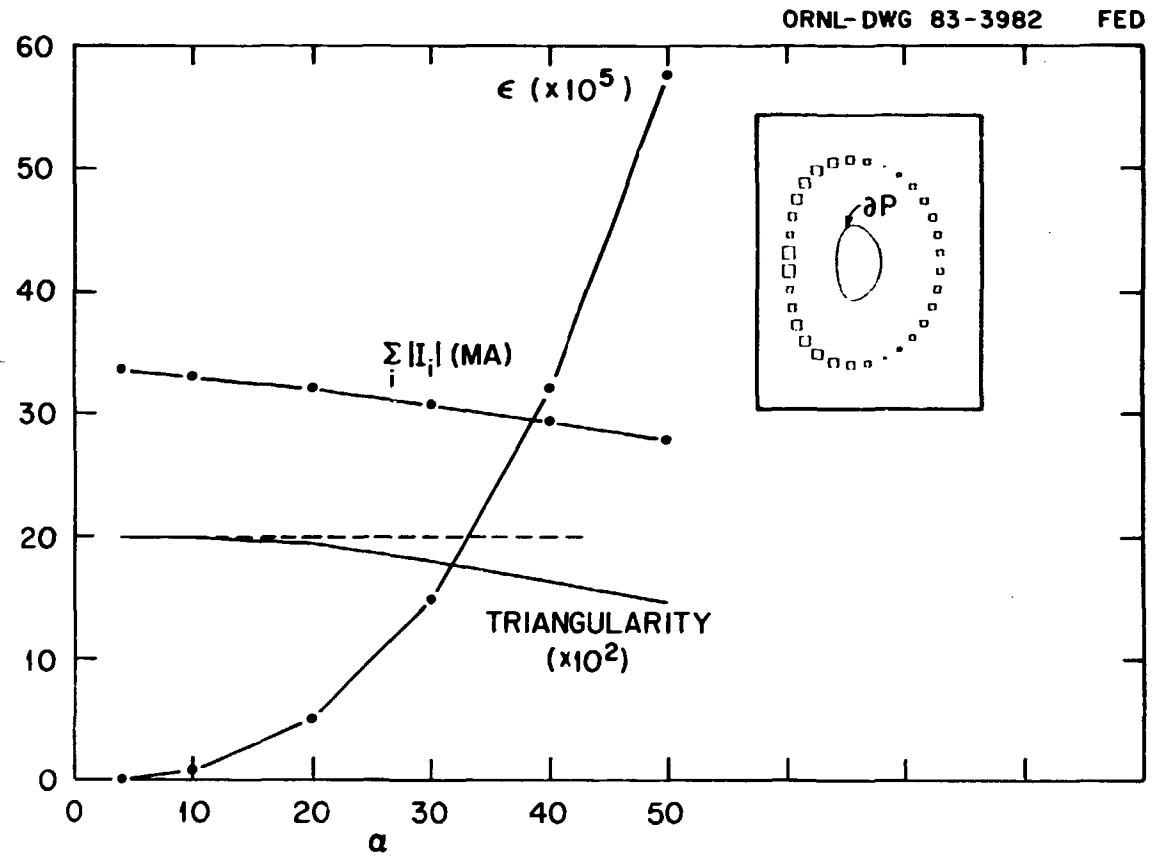

Fig. 3. Dependence of the relative error (ϵ) in flux values at the prescribed plasma boundary ∂P, total coil current, and triangularity on increasing α (Eq. 5).

A and B. These values are not unique [i.e., for each value of β_J, a set of parameters (A,B) exist for which $q_o = 1.0$ and $q_L = 2.0$, as shown in Fig. 4]. The optimization procedure converges to different points, depending on starting values (A,B) for fixed safety factor at the edge, which leaves some freedom for choice of profile shape.

In this PF analysis, different points in the time-dependent plasma operation scenario are simulated by equilibria with specific properties. For example, equilibria representing the plasma at the initiation and at the end of the burn interval are required to have constant shape, plasma current, and beta and to meet some flux swing requirement. This volt-second requirement takes the form

$$\Delta\Phi_{PF} = \Delta\Phi_{RES} + \Delta\Phi_{IND} \quad (7)$$

representing the balance between the externally applied flux due to the PF system and the resistive and inductive plasma flux requirements. The flux $\Delta\Phi_{PF}$ is computed from two equilibrium solutions with different fixed currents, usually in coils modeling the OH solenoid, as

$$\Delta\Phi_{PF} = \sum_i \Delta(M_{ip} I_i) \quad . \quad (8)$$

Here, M_{ip} is the mutual inductance between the i^{th} coil and the plasma and is computed in the FEDC equilibrium code as

$$M_{ip} = \sum_j M_{ip_j} J_{\phi_j} / \sum_j J_{\phi_j} \quad , \quad (9)$$

where J_{ϕ_j} is the current density at the j^{th} node in the solution of Eq. (1), and M_{ip_j} is the mutual inductance between axisymmetric current loops (filaments) at the center of coil i and at node j [4]. This model therefore accounts for changes in inductance due to a shift in the current profile during, for example, heating to high beta.

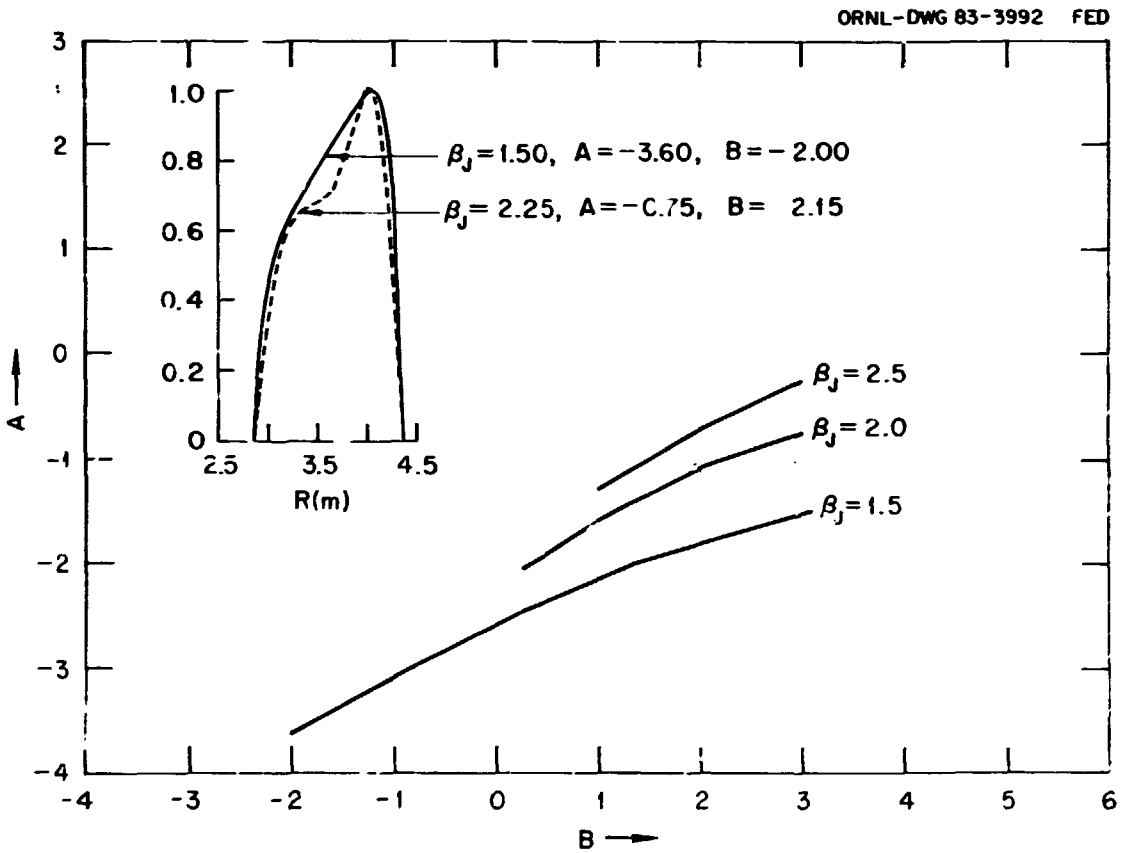

Fig. 4. Contours of constant axis and limiter values of q (q_o = 1.0, q_L = 2.0) in the profile parameters A and B (Eq. 6) for plasma parameters in the range of TFCX options (R_o = 3.6 m, a = 0.75 m, κ = 1.6, δ = 0.3 and B_t = 7.0 T). Current profiles (insert) vary along these contours.

2.3 PLASMA FLUX REQUIREMENTS

The volt-second requirements for inducing and maintaining the plasma current through the various stages of a discharge [Eq. (7)] include components accounting for resistive losses, $\Delta\Phi_{RES}$, and plasma inductance, $\Delta\Phi_{IND}$. The resistive term is given by

$$\Delta\Phi_{RES} = \int_{t_o}^{t_1} R_p I_p \, dt \, , \tag{10}$$

with the plasma resistance expressed as follows (mks units with T_e in keV):

$$R_p = \frac{3.3 \times 10^{-9} \, \alpha_N Z_{eff} R_o \ln \Lambda}{a^2 \kappa T_e^{3/2}} \, , \tag{11}$$

$$\ln \Lambda = 37.8 - \ln(n_e^{1/2}/T_e) \, .$$

Here, the factors $\alpha_N = 2$ and $Z_{eff} = 1.5$ are assumed to account for trapped electron effects and impurities, respectively. For the inductive component, the large aspect ratio approximation

$$\Delta\Phi_{IND} = \Delta(L_p I_p)$$

and

$$L_p = \mu R_o \left[\ln\left(\frac{8R_o}{a\kappa^{1/2}}\right) + \frac{\ell_i}{2} - 2 \right] \, , \tag{12}$$

with a correction for noncircularity ($1/\kappa^{1/2}$ in the logarithmic argument), is assumed. Here, ℓ_i is the plasma internal inductance.

2.4 PLASMA SCRAPEOFF CONSIDERATIONS

For elongated plasmas ($\kappa \sim 1.6$) of even moderate triangularity ($\delta \sim 0.2$–0.3), the shape of field lines in the scrapeoff region (i.e., flux surfaces immediately outside the limiter flux surface, $\psi = \psi_L$) is of particular interest in PF configuration design. The size of this region is dependent on plasma density and temperature profiles, but for design purposes it is generally assumed to have a width of about 5% of the plasma minor radius along the midplane on the large major radius side. For high-beta equilibria, where flux surfaces are considerably expanded on the small major radius side of the plasma, the inboard scrapeoff width can be a factor of 2 to 3 larger. The shape of this region has an influence on the design of tokamak components, such as the first wall and impurity control systems.

Figure 5 demonstrates a potential problem with highly elongated and D-shaped plasma cross sections. Significantly, the null point lies within the scrapeoff region and causes part of the region to be disconnected in the sense that some fraction of the field lines in the scrapeoff are diverted outside of the plasma chamber. This is a problem in tokamak designs that assume a pumped limiter or a single-null poloidal divertor as a means of impurity control.

Broad current profiles, characteristic of TFCX with $q_L = 2.0$, are desirable for increased scrapeoff width. A further improvement can be realized through optimization of the plasma shape. For an idealized PF coil system consisting of a large number of equally spaced conductors, implying precise plasma shaping capability, this is demonstrated by considering two different parameterizations of the plasma boundary shape given by the radial coordinates

$$R_i^{(1)} = R_o + a \cos(\theta_i + \delta \sin \theta_i) \tag{13}$$

and

$$R_i^{(2)} = R_o + a(\cos \theta_i + \sigma \cos 2\theta_i - \sigma) \tag{14}$$

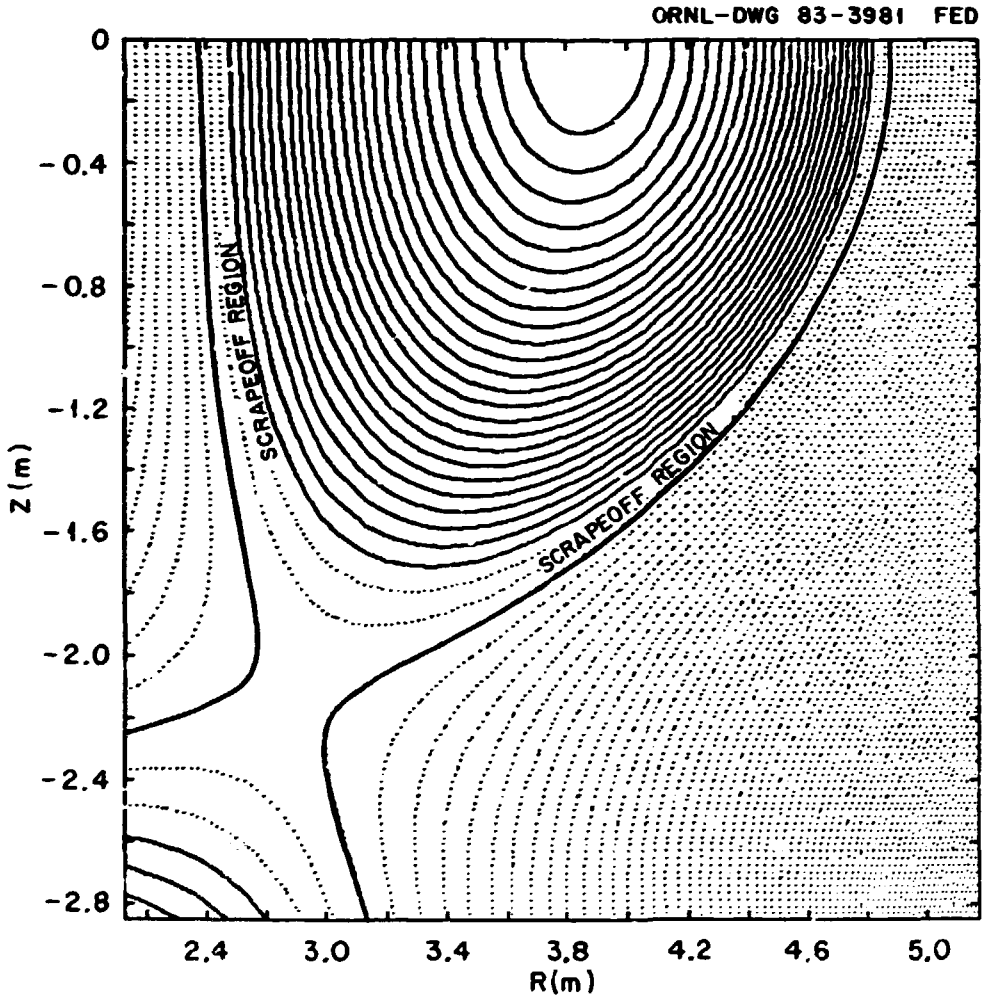

Fig. 5. Some fraction of the field lines in the scrapeoff region may be diverted outside the plasma chamber in highly elongated and D-shaped plasmas.

and the vertical coordinates $Z_i^{(1)} = Z_i^{(2)} = a\kappa \sin \theta_i$. Comparing the scrapeoff regions of equilibria with the same elongation ($\kappa = 1.60$) and triangularity ($\delta = 0.38$) as in Fig. 6, the boundary shape given by Eq. (14) is slightly more rounded, resulting in a broader scrapeoff.

In practice, however, these detailed shapes would require a more complex PF coil configuration, and a better solution may be to simply reduce the elongation or triangularity of the plasma, depending on the implications in terms of plasma performance [8]. In the analysis of TFCX coupled PF coil systems, plasmas with elongation $\kappa = 1.6$ and triangularity $\delta = 0.3$ seem to, at best, marginally satisfy the scrapeoff width requirements of a pumped limiter approach to impurity control.

3. POLOIDAL COIL DESIGN OPTIONS FOR TFCX

3.1 IMPACT ON SYSTEM TRADE STUDIES

Trade studies are under way to choose an appropriate concept for the TFCX conceptual design. The goal of these studies is to determine the sensitivity of machine size, cost, and performance to such design factors as plasma triangularity, maximum field strength at the TF coils, safety factor, and ignition parameter. The procedure through which the various design points are derived is heavily dependent on the PF coil design process described in Sect. 2. This model allows the evaluation of different concepts to be made based on a consistent set of criteria.

Although the details of the trade and evaluation studies (many of which are still in progress) are presented in ref. [1], the characteristics of the PF systems of the reference design points (TFCX-S and TFCX-H) are summarized here. In general, the size of devices increases with maximum field at the TF coils due to higher shielding requirements, larger TF coil widths, and smaller plasma minor radii, forcing the external PF coils to be further away from the plasma boundary. For fixed plasma shape, this enhanced distance increases shaping coil currents and, in turn, the fields at the SF coils, driving the machine design to a larger major radius.

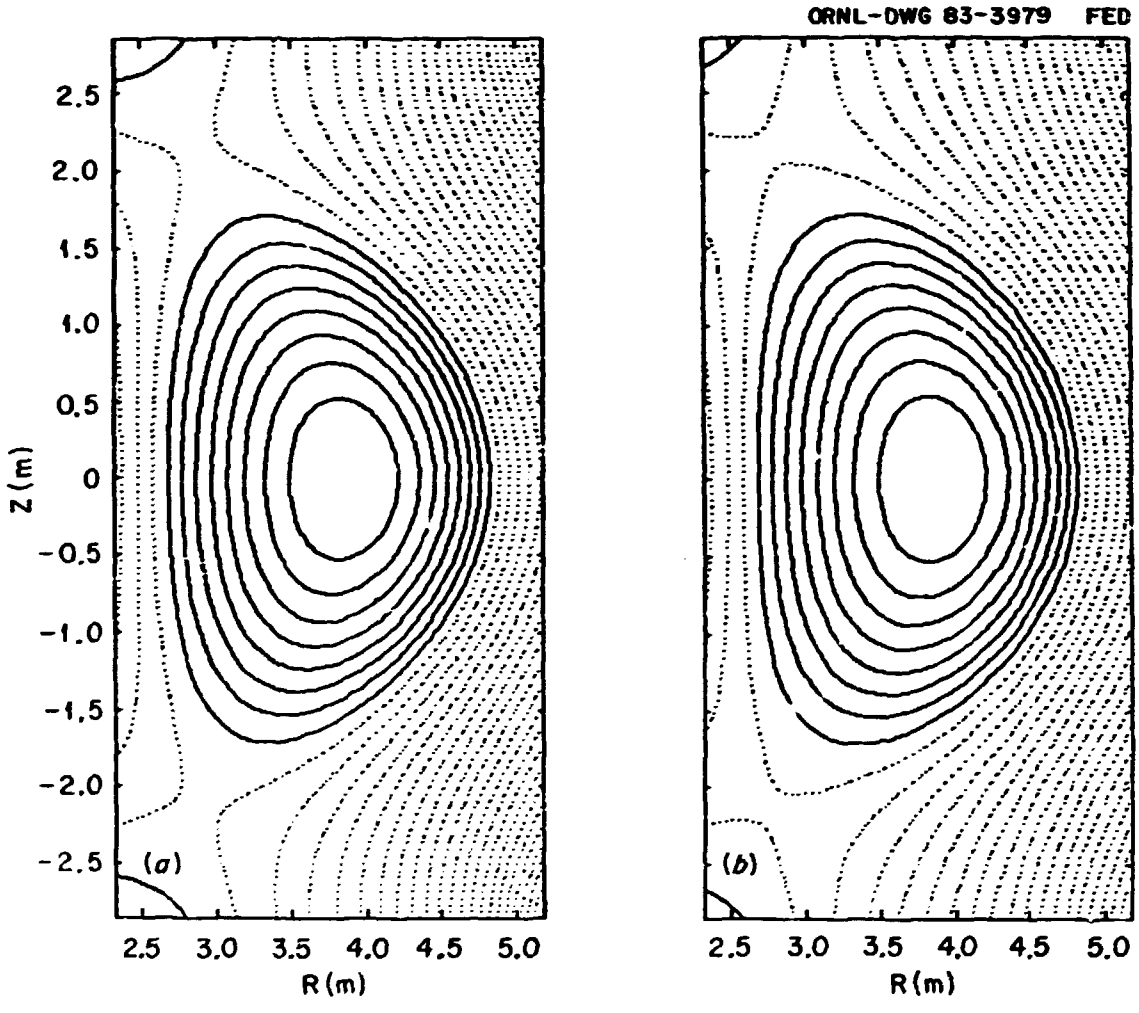

Fig. 6. For plasma cross sections of the same elongation (κ = 1.60) and triangularity (δ = 0.38), the sensitivity of the shape of field lines in the plasma scrapeoff region to different boundary shape parameterizations is shown using (a) Eq. (13) and (b) Eq. (14).

In the hybrid devices, a fixed plasma triangularity of $\delta = 0.3$ implies even larger major radii. Here OH solenoid currents in the same direction as the plasma current, needed to satisfy plasma volt-second requirements, combine additively with large SF coil currents to create excessive fields at the SF coils. The result is that to satisfy the field limits, the plasma and OH solenoid radii are so large that volt-seconds for a 300-s burn are satisfied with only a partial discharge of the OH solenoid. That is, the OH current runs counter to the plasma current, reducing fields at the SF coils and assisting in plasma shaping during the entire burn.

3.2 TFCX-S

The proposed all-SC coil reference point device for trade studies (TFCX-S) assumes a maximum field of 10 T at the TF coils. Following the design process of Sect. 2, a major radius of $R_o = 3.75$ m was found to be minimum with respect to satisfying the four PF system requirements listed in Sect. 1. Configurations at smaller radii satisfied maximum field constraints at the SF coils only when $\delta < 0.3$. At $R_o = 3.75$ m, the systems code analysis resulted in the plasma and design parameters listed in Table 1.

The OH solenoid and outboard EF coil locations are generally fixed by device radial build and access considerations. The SF coil locations are varied within the constraints of the configuration to satisfy the plasma shape requirement at the initiation of burn. With a coupled coil system, it is usually most difficult to shape the plasma when the current in the OH solenoid is either near zero or in the same direction as the plasma current. A summary of coil locations, currents, and volt-seconds is given in Table 2 for equilibria simulating the initiation and end of the 300-s burn pulse. The associated equilibrium plasma parameters are listed in Table 3. Figure 7 shows the TFCX-S high-beta equilibrium poloidal flux surfaces.

Table 1. TFCX-S data from systems code

Parameter	Value
Major radius (m)	3.75
Minor radius (m)	1.07
Field on-axis (T)	4.34
Beta, volume averaged (%)	5.9
Plasma current (MA)	7.70
Safety factor–axis	1.00
Safety factor–edge	2.00
Loop voltage (V)	0.06
Bucking cylinder inner radius (m)	0.87

Table 2. TFCX-S coil locations and currents

Coil	Mean radius, R_m (m)	Mean distance,[a] Z_m (m)	t = 40 s (start of burn) (MA-turn)	t = 340 s (end of burn) (MA-turn)	t = 40 s (start of burn) (V-s)	t = 340 s (end of burn) (V-s)	Δt = 300 s (during burn) (V-s)
1	1.50	3.50	9.34	5.00	4.31	2.31	-2.00
2	1.50	-3.50	9.34	5.00	4.31	2.31	-2.00
3	2.60	4.20	9.34	8.26	8.91	7.88	-1.03
4	2.60	-4.20	9.34	8.26	8.91	7.88	-1.03
5	6.70	3.50	-6.16	-6.45	-18.43	-19.31	-0.88
6	6.70	-3.50	-6.16	-6.45	-18.43	-19.31	-0.88
7	0.66	[b]	23.62	-28.37	4.42	-5.30	-9.72
			73.30[c]	67.79[c]	-5.99	-23.54	-17.55

[a] Values refer to mean distance from plasma midplane.

[b] Equal current centers at Z = ±0.20, ±0.60, ±1.00, ±1.40, ±1.80, and ±2.20 m.

[c] Sum of absolute currents.

Table 3. TFCX-S plasma parameters

Parameter	t = 40 s	t = 340 s
Major radius (m)	3.75	3.75
Minor radius (m)	1.07	1.07
Beta, volume averaged (%)	6.09	6.06
Plasma current (MA)	7.70	7.70
Safety factor–axis	0.95	0.95
Safety factor–edge	1.96	1.98
Elongation	1.60	1.60
Upper triangularity	0.30	0.30
Lower triangularity	0.30	0.30
Volt-seconds (resistive)	17.1	
Volt-seconds (PF system)	17.5	

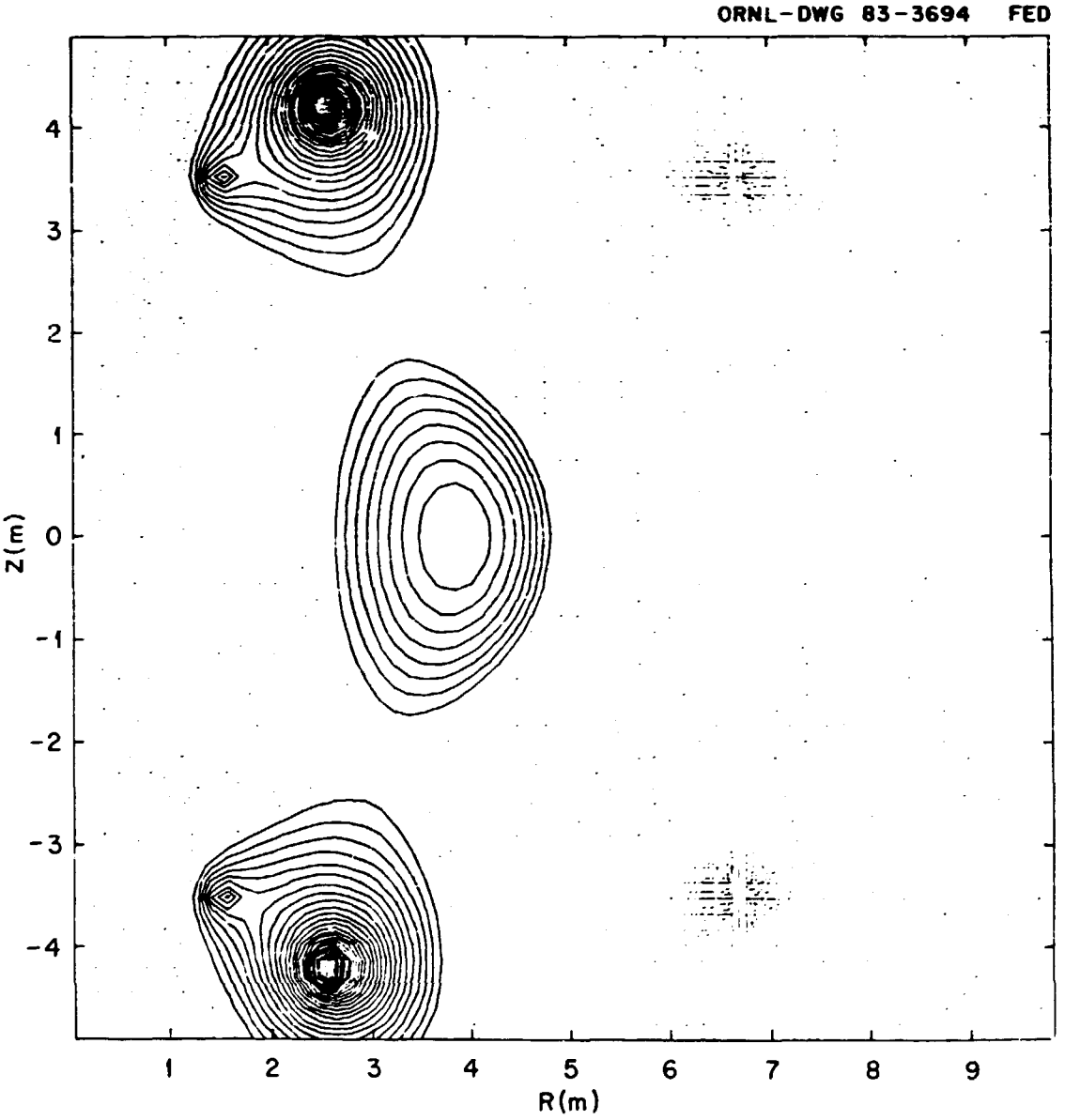

Fig. 7. High beta (<β> = 6.1%) TFCX-S equilibrium poloidal flux surfaces for a fully discharged OH solenoid (I_{OH} = -28 MA) at the end of burn t = t_F.

3.3 TFCX-H

The proposed reference device for the hybrid concept (TFCX-H) assumes superconducting TF coils with a maximum field of 8 T, together with copper-insert TF coils providing for an increased field on-axis. The minimum major radius (R_o = 3.6 m) satisfying PF system requirements is again limited by the triangularity condition in the sense that designs of smaller major radius exceed the 8-T PF constraint at the SF coils when δ = 0.3. The data from the systems code analysis at this radius are given in Table 4, followed by the results of the equilibrium analysis in Tables 5 and 6. Figures 8 and 9 show the TFCX-H coil locations and typical high-beta poloidal flux surfaces.

In previous tokamak designs, the OH solenoid current has been assumed to discharge from some maximum value to the same current in the opposite direction. When maximum fields in the SC coils are taken into consideration, design configurations of smaller major radii are possible when the solenoid is allowed to discharge asymmetrically. For the TFCX-H at R_o = 3.6 m, volt-seconds during burn ($\Delta\Phi$ = -19.4 V-s) are due mainly to the solenoid swing ($\Delta\Phi_{OH}$ = -10.9 V-s) and are provided by starting the solenoid at the initiation of burn with zero current [$I_{OH}(t_I)$ = 0 MA] and ramping it down to $I_{OH}(t_F)$ = -30.24 MA.

4. POLOIDAL COIL CURRENT SCENARIOS FOR THE TFCX

4.1 PLASMA STARTUP

Options under consideration for TFCX current initiation and startup include totally rf startup (current drive) and rf-assisted (partially inductive) startup. The implications in terms of the PF system have to do mainly with the OH solenoid current waveform.

The TFCX startup scenario is based on the assumption of major radius compression with the plasma growing in minor radius while in contact with an outboard limiter [9]. The plasma current and SF coil currents are preprogrammed to increase linearly from values consistent with a circular plasma immediately following current initiation to

Table 4. TFCX-H data from systems code

Parameter	Value
Major radius (m)	3.60
Minor radius (m)	0.97
Field on-axis (T)	4.[illegible]
Beta, volume averaged (%)	5.6
Plasma current (MA)	7.23
Safety factor–axis	1.00
Safety factor–edge	2.00
Loop voltage (V)	0.06
Bucking cylinder inner radius (m)	1.12

Table 5. TFCX-H coil locations and currents

Coil	Mean radius, R_m (m)	Mean distance,[a] Z_m (m)	t = 40 s (start of burn)	t = 340 s (end of burn)	t = 40 s (start of burn)	t = 340 s (end of burn)	Δt = 300 s (during burn)
			(MA-turns)		(V-s)		
1	1.70	3.30	7.05	2.75	4.36	1.70	-2.66
2	1.70	-3.64	9.39	2.75	5.05	1.48	-3.57
3	2.65	3.85	7.05	6.70	7.64	7.26	-0.38
4	2.65	-4.19	9.39	9.98	8.86	9.41	0.55
5	6.23	3.20	-5.85	-6.26	-17.42	-18.63	-1.21
6	6.23	-3.54	-7.25	-7.69	-19.81	-21.02	-1.21
7	0.90	*b*	0.00	-30.24	0.00	-10.93	-10.93
			45.98[c]	66.36[c]	-11.32	-30.73	-19.41

[a] Values refer to mean distance from plasma midplane.

[b] Equal current centers at Z = ±0.20, ±0.60, ±1.00, ±1.40, ±1.80, and ±2.20 m.

[c] Sum of absolute currents.

Table 6. TFCX-H plasma parameters

Parameter	t = 40 s	t = 340 s
Major radius (m)	3.60	3.60
Minor radius (m)	0.97	0.97
Beta, volume averaged (%)	5.29	5.27
Plasma current (MA)	7.23	7.23
Safety factor–axis	0.97	0.97
Safety factor–edge	1.96	1.97
Elongation	1.60	1.60
Upper triangularity	0.30	0.30
Lower triangularity	0.30	0.30
Volt-seconds (resistive)	18.9	
Volt-seconds (PF system)	19.4	

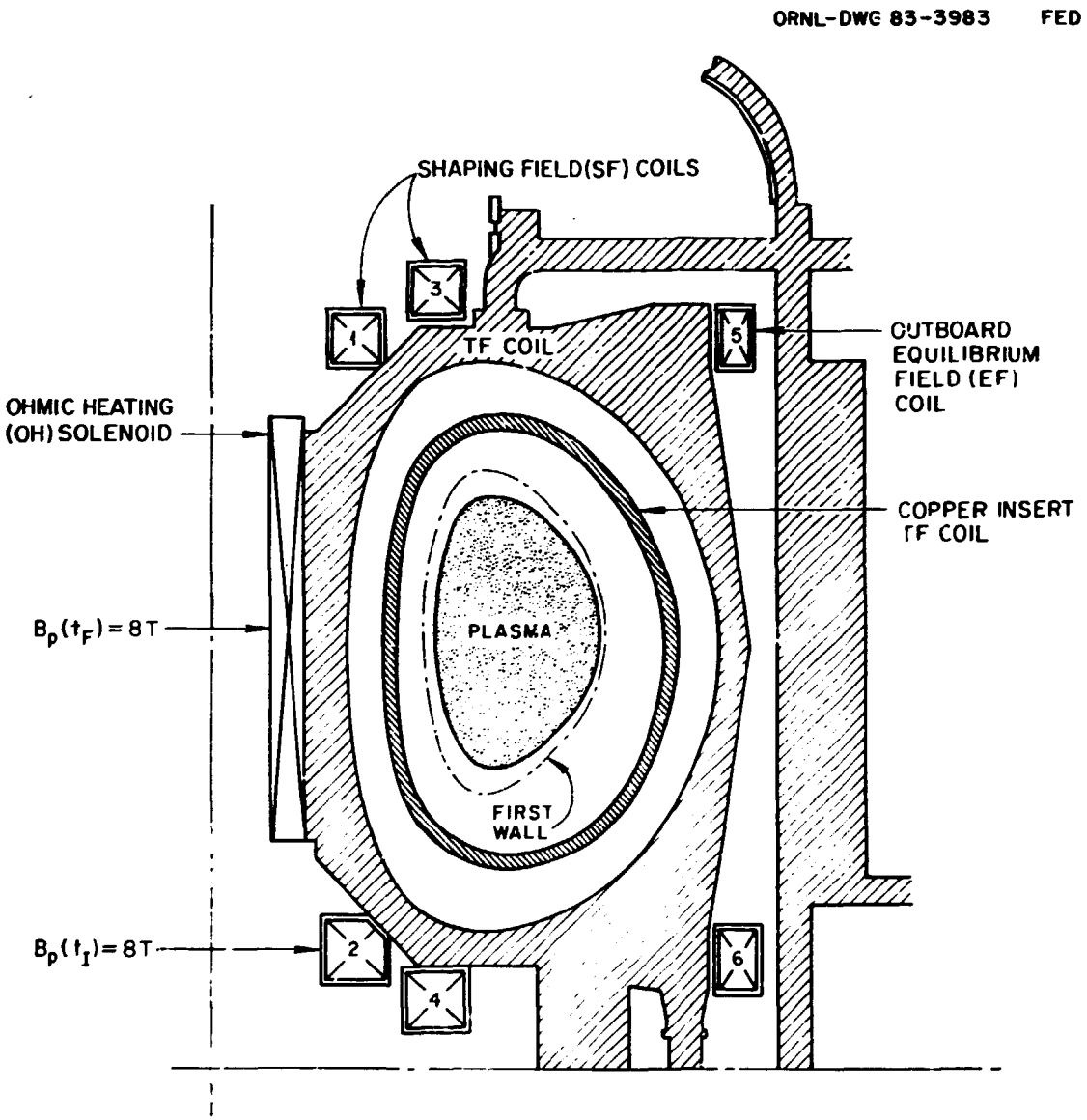

Fig. 8. The TFCX-H poloidal field coil system.

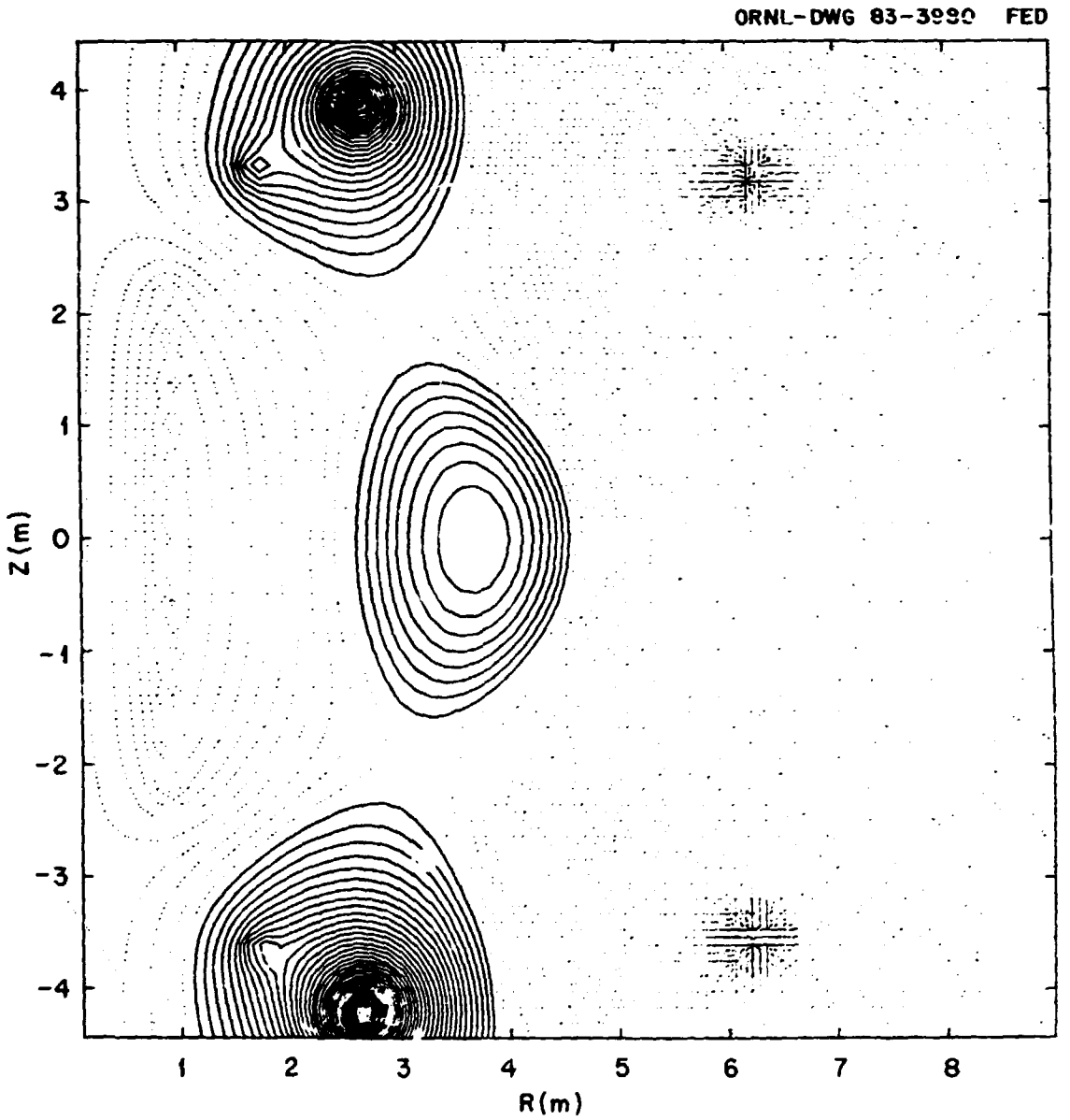

Fig. 9. High beta (<β> = 5.3%) TFCX-H equilibrium poloidal flux surfaces for a fully discharged OH solenoid (I_{OH} = -30 MA) at the end of burn $t = t_F$.

those of a low-beta, elongated, and D-shaped plasma (κ = 1.6, δ = 0.2) prior to bulk heating. Outboard EF coil currents are determined such that q = 2.0 is maintained at the plasma edge during the minor radius expansion.

For the case of totally rf startup, a steady-state OH solenoid current is maintained at a level defined by the flux requirements during bulk heating to high beta and at the initiation of burn. For partially inductive startup, the OH solenoid is discharged from some maximum current to zero current in 2 s, then recharged to a level consistent with flux requirements during auxiliary heating and at the initiation of burn. In either case, the only startup current waveform to be computed with the equilibrium code is that of the outer EF coils.

Assuming a 30-s interval for totally rf current initiation and startup, plasma parameters and PF coil currents for TFCX-S and TFCX-H at t = 1, 2, 10, 20, and 30 s into a discharge are given in Tables 7–10 and in Figs. 10 and 11. The parameters and coil currents for TFCX-S, assuming an rf-assisted startup, are given for t = 1, 2, 10, and 20 s in Tables 11 and 12. The current waveforms for an rf-assisted startup scenario on TFCX-S are shown in Fig. 12. In these calculations, the current in the copper-insert TF coils produces about 1.4 T on-axis and is assumed to be constant during startup.

4.2 PLASMA HEATING

Plasma bulk heating on TFCX is characterized, for the purpose of PF system design, by an assumed linear increase in electron temperature (i.e., an increase in beta) from 1.5 to 13.0 keV over a 10-s interval. Using Eqs. (10)–(12), the resistive plus inductive flux requirements for TFCX-S and TFCX-H are approximately $\Delta\Phi$ = -5.9 V-s and $\Delta\Phi$ = -5.1 V-s, respectively. Meeting these values with the externally applied flux due to the PF coils actually requires a slight recharge of the OH solenoid current because the outward shift of the plasma current profile during the transition to high beta better couples the plasma column to the outboard EF coils, producing more than the necessary flux swing.

PF coil current waveforms and flux swing capability for TFCX-S and TFCX-H (for a 300-s inductive burn) are shown in Figs. 10 and 11.

Table 7. TFCX-S coil currents for totally rf startup

	Coil						
	OH	1	2	3	4	5	6
	Radius, R (m)						
	0.66	1.50	1.50	2.60	6.70	6.70	6.70
	Distance from plasma midplane, Z (m)						
	a	3.50	-3.50	4.20	-4.20	3.50	-3.50
	Current (MA-turns)						
t = 1 s	20.64	0.64	0.64	0.64	0.64	-0.21	-0.21
t = 2 s	20.64	0.91	0.91	0.91	0.91	-0.37	-0.37
t = 10 s	20.64	3.20	3.20	3.20	3.20	-1.70	-1.70
t = 20 s	20.64	6.09	6.09	6.09	6.09	-3.42	-3.42
t = 30 s	20.64	9.10	9.10	9.10	9.10	-5.09	-5.09
t = 40 s	23.62	9.34	9.34	9.34	9.34	-6.16	-6.16
t = 340 s	-28.37	5.00	5.00	8.26	8.26	-6.45	-6.45

[a]Equal current centers at Z = ±0.20, ±0.60, ±1.00, ±1.40, ±1.80, and ±2.20 m.

Table 8. TFCX-S plasma parameters for totally rf startup

Time (s)	R_o (m)	a (m)	Elongation	Triangularity	I_p (MA)	<β> (%)	ϕ (V-s)[a]
1	4.38	0.44	1.00	0.00	0.48	0.03	3.94
2	4.30	0.52	1.01	0.01	0.70	0.05	3.63
10	3.95	0.87	1.15	0.06	2.55	0.14	2.17
20	3.80	1.02	1.36	0.14	4.89	0.72	0.64
30	3.75	1.07	1.60	0.25	7.27	1.19	-0.01
40	3.75	1.07	1.60	0.30	7.70	6.09	-5.99
340	3.75	1.07	1.60	0.30	7.70	6.0(	-23.54

[a] ϕ (V-s) = $\sum_i M_{ip} I_i$.

Table 9. TFCX-H coil currents for totally rf startup

	Coil						
	OH	1	2	3	4	5	6
	Radius, R (m)						
	0.90	1.70	1.70	2.65	2.65	6.23	6.23
	Distance from plasma midplane, Z (m)						
	a	3.30	-3.64	3.85	-4.19	3.20	-3.54
	Current (MA-turns)						
t = 1 s	-1.98	-0.16	-0.16	-0.16	-0.16	-0.37	-0.42
t = 2 s	-1.98	0.08	0.17	0.08	0.17	-0.52	-0.62
t = 10 s	-1.98	2.02	2.76	2.02	2.76	-1.76	-2.22
t = 20 s	-1.98	4.49	6.01	4.49	6.01	-3.38	-4.27
t = 30 s	-1.98	6.96	9.22	6.96	9.22	-4.95	-6.22
t = 40 s	0.00	7.05	9.39	7.05	9.39	-5.85	-7.25
t = 340 s	-30.24	2.75	2.75	6.70	9.98	-6.26	-7.69

[a]Equal current centers at Z = ±0.20, ±0.60, ±1.00, ±1.40, ±1.80, and ±2.20 m.

Table 10. TFCX-H plasma parameters for totally rf startup

Time (s)	R_o (m)	a (m)	Elongation	Triangularity[a]	I_p (MA)	<β> (%)	φ (V-s)[b]
1	4.14	0.43	1.00	0.00	0.54	0.03	-3.94
2	4.01	0.50	1.01	0.01	0.76	0.05	-4.14
10	3.77	0.80	1.16	0.06	2.51	0.17	-5.02
20	3.64	0.9[illegible]	1.38	0.15	4.72	0.58	-5.85
30	3.60	0.97	1.60	0.25	6.95	0.96	-6.19
40	3.60	0.97	1.60	0.30	7.23	5.29	-11.32
340	3.60	0.97	1.60	0.30	7.23	5.27	-30.73

[a] Average of upper and lower triangularity.

[b] ϕ (V-s) = $\sum_i M_{ip} I_i$.

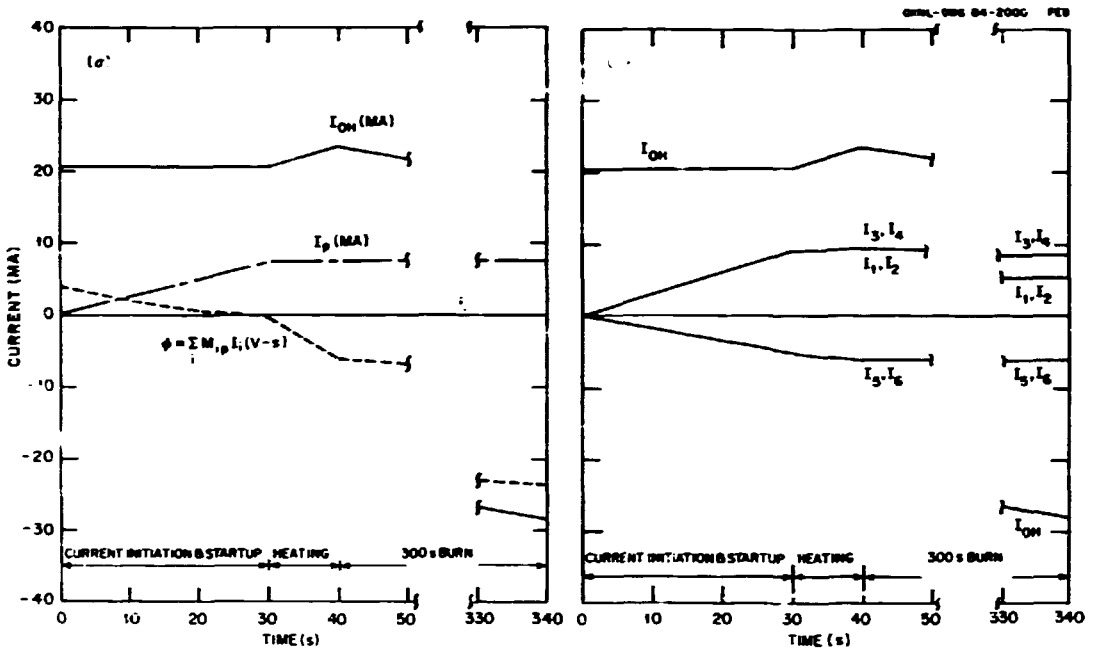

Fig. 10. TFCX-S: (a) plasma, OH current, volt-seconds and (b) poloidal coil current waveforms for totally rf startup.

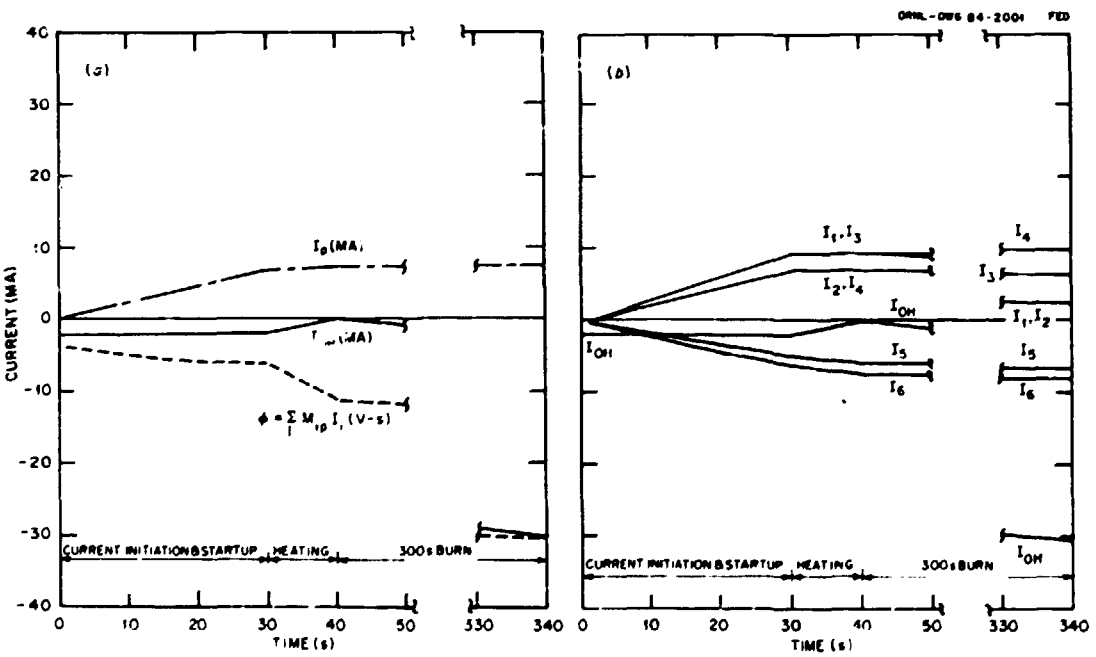

Fig. 11. TFCX-H: (a) plasma, OH current, volt-seconds and (b) poloidal coil current waveforms for totally rf startup.

Table 11. TFCX-S coil currents for rf-assisted startup

	Coil						
	OH	1	2	3	4	5	6
	Radius, R (m)						
	0.66	1.50	1.50	2.60	2.60	6.70	6.70
	Distance from plasma midplane, Z (m)						
	a	3.50	-3.50	4.20	-4.20	3.50	-3.50
	Current (MA-turns)						
t = 1 s	14.16	0.41	0.41	0.41	0.41	-0.24	-0.24
t = 2 s	0.00	0.10	0.10	0.10	0.10	-0.47	-0.47
t = 10 s	5.76	2.58	2.58	2.58	2.58	-1.76	-1.76
t = 20 s	13.20	5.79	5.79	5.79	5.79	-3.45	-3.45
t = 30 s[b]	20.64	9.10	9.10	9.10	9.10	-5.09	-5.09

[a]Equal current centers at Z = ±0.20, ±0.60, ±1.00, ±1.40, ±1.80, and ±2.20 m.

[b]Values at t = 30, 40, and 340 s are the same as in Table 7.

Table 12. TFCX-S plasma parameters for rf-assisted startup

Time (s)	R_o (m)	a (m)	Elongation	Triangularity	I_p (MA)	$\langle\beta\rangle$ (%)	ϕ (V-s)[a]
1	4.38	0.44	1.00	0.00	0.48	0.03	1.87
2	4.30	0.52	1.01	0.01	0.70	0.05	-3.12
10	3.95	0.87	1.15	0.06	2.55	0.19	-2.75
20	3.80	1.02	1.36	0.14	4.89	0.72	-1.80
30[b]	3.75	1.07	1.60	0.25	7.27	1.19	-0.01

[a] ϕ (V-s) = $\sum_i M_{ip} I_i$.

[b] Values at t = 30, 40, and 340 s are the same as in Table 9.

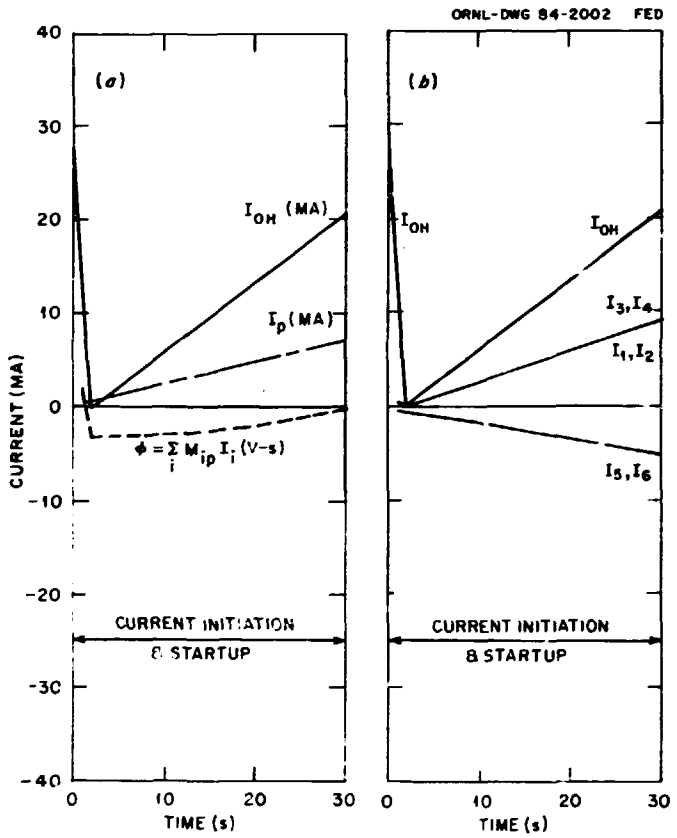

Fig. 12. TFCX-S: (a) plasma, OH current, and volts-seconds waveforms for rf-assisted startup and (b) poloidal coil currents.

4.3 QUASI-STEADY-STATE OPERATION

The pulsed nature of an inductively driven tokamak tends to limit its lifetime and availability through the effects of large cyclic electromagnetic forces. The assumption of successful rf current drive at relatively low density leads to the possibility of demonstrating (on TFCX) a quasi-steady-state mode of operation in which the plasma current is maintained at some substantial level as the solenoid current is periodically recharged. The changes in the PF coil current waveforms necessary to accommodate such an operating scenario are discussed in this section.

The TFCX is designed such that the application of its full OH induction flux capability at high beta (i.e., subject to the constraints imposed by maximum fields at the PF coils) results in a 300-s burn. This burn phase will have to be shortened somewhat for cyclic operation in order to reserve sufficient volt-seconds for a plasma cool-down phase. During heating, the outward shift of the plasma current profile contributes to the flux due to the PF system ($\Delta\Phi_{PF}$), but during cool-down the mutual coupling between the plasma and the outer EF coils decreases. This flux loss, together with the required $\Delta\Phi = \Delta\Phi_{RES} + \Delta\Phi_{IND}$, must be overcome through some OH solenoid swing.

Because there is about a 5% decrease in plasma current during cooling, $\Delta\Phi_{IND}$ changes sign relative to its value during heating, and the approximate flux requirements for a 10-s cool-down period on TFCX-S total $\Delta\Phi$ = 1.1 V-s. This implies a maximum burn cycle of ~160 s; the resulting current waveforms for quasi-steady-state operation of TFCX-S are presented in Fig. 13.

5. SUMMARY AND CONCLUSIONS

The FEDC equilibrium code is used, together with the EFFI magnetics code, to determine the feasibility of tokamak configurations with respect to poloidal magnetics requirements in the preconceptual design of the TFCX. Given an operating point defined in an FEDC tokamak

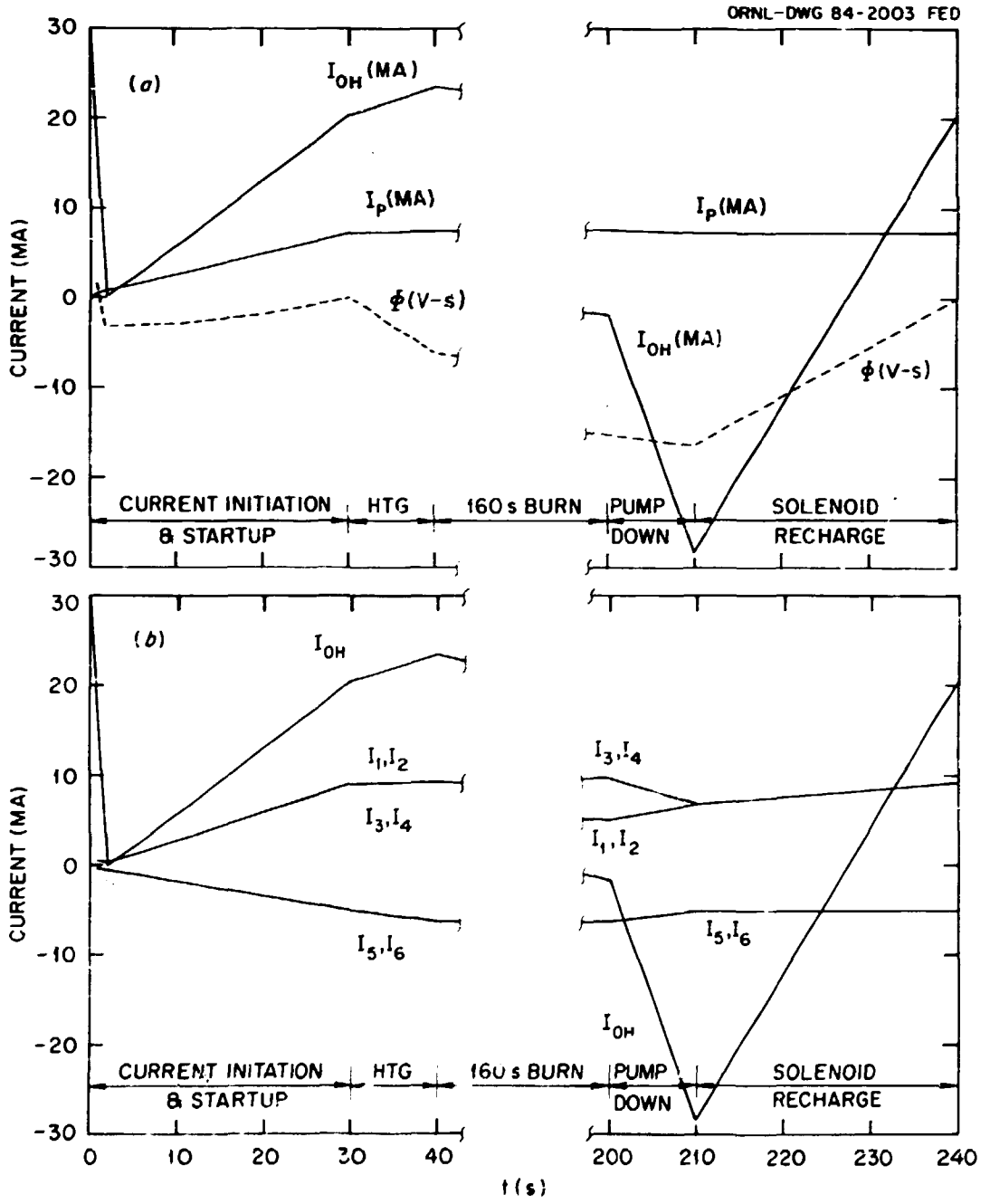

Fig. 13. TFCX-S: (a) OH solenoid current (I_{OH}), plasma current (I_p), and volt-second (Φ) waveforms and (b) OH solenoid current (I_{OH}), shaping field current (I_{SF}), and outboard equilibrium field coil current (I_{EF}) for quasi-steady-state operation.

systems code analysis, these computational tools are used to locate PF coils with respect to mechanical and magnetic constraints, while attempting to satisfy plasma flux and shape requirements. Simultaneously satisfying these constraints and performance criteria indicates that the PF system has a great impact on machine size. In particular, fixed plasma shape may make it difficult to obtain objective comparisons among different TFCX concepts. Trade studies, using the PF system design process discussed in Sect. 2, are under way to determine the dependence of machine cost and size on plasma shape and other performance factors.

PF coil locations and current waveforms are presented for the reference design points of two possible options (TFCX-S and TFCX-H), both with minimum major radius and both satisfying the PF requirements. It is demonstrated that plasma scrapeoff considerations may place upper bounds on TFCX shaping parameters under present impurity control system assumptions. Finally, coil currents consistent with equilibrium and volt-second requirements are given for TFCX startup and for a possible scenario of quasi-steady-state operation. The burn time during each cycle in a quasi-steady-state mode will have to be considerably shorter than 300 s in order to reserve a sufficient OH solenoid current swing to inductively maintain the plasma current during a cool-down period prior to solenoid recharge.

REFERENCES

[1] C. A. Flanagan et al., *Toroidal Fusion Core Experiment: Design Studies Based on Superconducting and Hybrid Toroidal Field Coils*, to be published at Oak Ridge National Laboratory.

[2] R. L. Reid and D. Steiner, "Parametric Studies for the Fusion Engineering Device," *Nucl. Technol./Fusion* 4, 120 (1983).

[3] S. J. Sackett, *EFFI-A Code for Calculating the Electromagnetic Field, Force, and Inductance in Coil Systems of Arbitrary Geometry*, UCRL-52402, Lawrence Livermore Laboratory, 1978.

[4] W. R. Smythe, *Static and Dynamic Electricity*, McGraw-Hill, New York, 1950.

[5] P. N. Swartztrauber and R. A. Sweet, "Algorithm 541. Efficient Fortran Subprograms for the Solution of Separable Elliptic Partial Differential Equations," *ACM Transactions on Mathematical Software* 5 (3), 352 (1979).

[6] D. J. Strickler, Y-K. M. Peng, and T. G. Brown, *Equilibrium Field Coil Concepts for INTOR*, ORNL/TM-7746, Oak Ridge Natl. Lab., 1981.

[7] R. L. Crane, K. E. Hillstrom, and M. Minkoff, *Solution of the General Nonlinear Programming Problem With the Subroutine VMCON*, ANL-80-64, Argonne National Laboratory, 1980.

[8] A. M. M. Todd et al., "Dependence of Ideal-MHD Kink and Ballooning Modes on Plasma Shape and Profiles in Tokamaks," *Nucl. Fusion* 19 (6), 743 (1979).

[9] S. K. Borowski, *Inductive Current Startup in Large Tokamaks With Expanding Minor Radius and RF Assist*, ORNL/FEDC-83/8, Fusion Engineering Design Center, Oak Ridge Natl. Lab., 1983.

ORNL/FEDC-83/10
Dist. Category UC-20 c,d

INTERNAL DISTRIBUTION

1. S. K. Borowski
2. R. D. Burris
3. B. Carreras
4. R. A. Dory
5. J. L. Dunlap
6. C. A. Flanagan
7. G. M. Fuller
8. G. E. Gorker
9. P. N. Haubenreich
10. S. S. Kalsi
11. J. Kirchner
12. C. M. Loring
13-17. J. B. Miller
18. J. A. O'Toole
19. Y-K. M. Peng
20. W. T. Reiersen
21-25. K. E. Rothe
26. P. H. Sager
27. M. J. Saltmarsh
28. J. Sheffield
29-33. D. J. Strickler
34. D. W. Swain
35. N. A. Uckan
36. J. B. Wilgen
37-38. Laboratory Records Department
39. Laboratory Records, ORNL-RC
40. Document Reference Section
41. Central Research Library
42. Fusion Energy Division Library
43. Fusion Energy Division Publications Office
44. ORNL Patent Office

EXTERNAL DISTRIBUTION

45. M. A. Abdou, Associate Director, FPP/207, Argonne National Laboratory, 9700 South Cass Avenue, Argonne, IL 60439
46. N. A. Amherd, Fusion Power Program, Advanced Systems Department, Electric Power Research Institute, P.O. Box 10412, Palo Alto, CA 94304
47. J. L. Anderson, CMB-3, Mail Stop 348, Los Alamos National Laboratory, P.O. Box 1663, Los Alamos, NM 87545
48. M. Anderson, Tennessee Valley Authority, 1300 Commerce Bank Building, Chattanooga, TN 37401
49. O. A. Anderson, Lawrence Berkeley Laboratory, University of California, Berkeley, CA 94720
50. D. J. Anthony, Advanced Power Program, Advanced Energy Programs Department, Building 2, Room 551, General Electric Company, Schenectady, NY 12345
51. C. C. Baker, FPP/208, Argonne National Laboratory, 9700 South Cass Avenue, Argonne, IL 60439
52. T. H. Batzer, L-536, Lawrence Livermore National Laboratory, P.O. Box 808, Livermore, CA 94550
53. J. E. Baublitz, Office of Fusion Energy, Office of Energy Research, Mail Station G-256, Department of Energy, Washington, DC 20545
54. W. Bauer, Physical Research Division, Sandia National Laboratories-Livermore, Livermore, CA 94550
55. J. F. Baur, GA Technologies, Inc., P.O. Box 81608, San Diego, CA 92138

56. D. S. Beard, Office of Fusion Energy, Office of Energy Research, Mail Stop G-256, U.S. Department of Energy, Washington, DC 20545
57. R. J. Beeley, ETEC, Rockwell International, P.O. Box 1449, Canoga Park, CA 91304
58. D. C. Berkey, Vice President & General Manager, Energy System and Technology Division, General Electric Company, P.O. Box 7600, Stamford, CT 06904
59. K. L. Black, Department E452, McDonnell Douglas Astronautics Company, P.O. Box 516, St. Louis, MO 63166
60. R. Botwin, C47-05, Grumman Aerospace Corporation, P.O. Box 31, Bethpage, NY 11714
61. W. B. Briggs, McDonnell Douglas Astronautics Company, P.O. Box 516, St. Louis, MO 63166
62. G. Bronner, Princeton Plasma Physics Laboratory, P.O. Box 451, Princeton, NJ 08544
63. J. N. Brooks, FPP/207, Argonne National Laboratory, 9700 South Cass Avenue, Argonne, IL 60439
64. S. C. Burnett, GA Technologies, Inc., P.O. Box 81608, San Diego, CA 92138
65. J. D. Callen, Department of Nuclear Engineering, University of Wisconsin, Madison, WI 53706
66. V. S. Chan, GA Technologies, Inc., P.O. Box 81608, San Diego, CA 92138
67. R. G. Clemmer, Fusion Power Program, Argonne National Laboratory, 9700 South Cass Avenue, Argonne, IL 60439
68. D. R. Cohn, MIT Plasma Fusion Center, 167 Albany Street, Cambridge, MA 02139
69. W. S. Cooper, Lawrence Berkeley Laboratory, University of California, Berkeley, CA 94720
70. J. W. Coursen, C36-05, Grumman Aerospace Corporation, P.O. Box 31, Bethpage, NY 11714
71. R. W. Conn, School of Chemical, Nuclear, and Thermal Engineering, Boelter Hall, University of California, Los Angeles, CA 90024
72. J. G. Crocker, EG&G Idaho, P.O. Box 1625, Idaho Falls, ID 83401
73. A. E. Dabiri, Energy Systems and Conservation Division, Science Applications, Inc., P.O. Box 2351, La Jolla, CA 92038
74. C. C. Damm, L-441, Lawrence Livermore National Laboratory, P.O. Box 808, Livermore, CA 94550
75. R. C. Davidson, Massachusetts Institute of Technology, 77 Massachusetts Avenue, Cambridge, MA 02139
76. N. A. Davies, Office of Fusion Energy, Office of Energy Research, Mail Station G-256, U.S. Department of Energy, Washington, DC 20545
77. J. W. Davis, E457, Building 81/1/B7, McDonnell Douglas Astronautics Company, P.O. Box 516, St. Louis, MO 63166
78. M. J. Davis, Sandia National Laboratories, P.O. Box 5800, Albuquerque, NM 87185
79. S. O. Dean, Director, Fusion Energy Development, Science Applications, Inc., 2 Professional Drive, Suite 249, Gaithersburg, MD 20760
80. J. F. Decker, Office of Fusion Energy, Department of Energy, Mail Stop G-256, Washington, DC 20545

81. D. DeFreece, E451, Building 81/1/B7, McDonnell Douglas Astronautics Company, P.O. Box 516, St. Louis, MO 63166
82. A. Deitz, Princeton Plasma Physics Laboratory, P.O. Box 451, Princeton, NJ 08544
83. D. A. Dingee, Program Manager, Fusion Technology, Pacific Northwest Laboratories, Battelle Boulevard, Richland, WA 99352
84. J. N. Doggett, L-441, Lawrence Livermore National Laboratory, P.O. Box 808, Livermore, CA 94550
85. H. Dreicer, Division Leader, CRT, Los Alamos National Laboratory, P.O. Box 1663, Los Alamos, NM 87545
86. D. Ehst, Argonne National Laboratory, 9700 South Cass Avenue, Argonne, IL 60439
87. G. A. Eliseev, I V. Kurchatov Institute of Atomic Energy, P.O. Box 3402, 123182 Moscow, U.S.S.R.
88. W. R. Ellis, Office of Fusion Energy, Department of Energy, Mail Stop G-256, Washington, DC 20545
89. B. A. Engholm, GA Technologies, Inc., P.O. Box 81608, San Diego, CA 92138
90. H. P. Eubank, Princeton Plasma Physics Laboratory, P.O. Box 451, Princeton, NJ 08544
91. F. Farfaletti-Casali, Engineering Division, Joint Research Center, Ispra Establishment, 21020 Ispra (Varese), Italy
92. J. J. Ferrante, Manager, Building 36-241, Large Superconducting Program, General Electric Company, 1 River Road, Schenectady, NY 12345
93. J. File, Princeton Plasma Physics Laboratory, P.O. Box 451, Princeton, NJ 08544
94. P. A. Finn, Fusion Power Program, Argonne National Laboratory, 9700 South Cass Avenue, Argonne, IL 60439
95. H. K. Forsen, Bechtel Group, Inc., Research & Engineering, P.O. Box 3965, San Francisco, CA 94119
96. J. S. Foster, Jr., Building R4-2004, TRW Defense and Space Systems, 1 Space Park, Redondo Beach, CA 90278
97. T. K. Fowler, Associate Director for MFE, L-436, Lawrence Livermore National Laboratory, P.O. Box 808, Livermore, CA 94550
98. J. W. French, EBASCO Services, Inc., Forrestal Campus, CN-59, Princeton University, Princeton, NJ 08544
99. H. P. Furth, Director, Princeton Plasma Physics Laboratory, P.O. Box 451, Princeton, NJ 08544
100. J. G. Gavin, Jr., President, A01-11, Grumman Aerospace Corporation, P.O. Box 31, Bethpage, NY 11714
101. G. Gibson, Westinghouse Electric Corporation, Fusion Power Systems Department, P.O. Box 10864, Pittsburgh, PA 15236
102. J. R. Gilleland, Manager, Fusion Project, GA Technologies, Inc., P.O. Box 81608, San Diego, CA 92138
103. V. A. Glukhikh, Scientific-Research Institute of Electro-Physical Apparatus, 188631 Leningrad, U.S.S.R.
104. M. Y. Gohar, Argonne National Laboratory, 9700 South Cass Avenue, Argonne, IL 60439
105. W. D. Goins, Tennessee Valley Authority, 1300 Commerce Union Bank Building, Chattanooga, TN 37401

106. D. A. Goldberg, Lawrence Berkeley Laboratory, University of California, Berkeley, CA 94720
107. R. Goldston, Princeton Plasma Physics Laboratory, P.O. Box 451, Princeton, NJ 08544
108. M. B. Gottlieb, Princeton Plasma Physics Laboratory, P.O. Box 451, Princeton, NJ 08544
109. R. W. Gould, Department of Applied Physics, California Institute of Technology, Pasadena, CA 91109
110. M. W. Griffin, Department E236, McDonnell Douglas Astronautics Company, P.O. Box 516, St. Louis, MO 63166
111. C. R. Head, Office of Fusion Energy, Department of Energy, Mail Stop G-256, Washington, DC 20545
112. W. Heinz, Institut fur Technische Physik, Kernforschungszentrum Karlsruhe GmbH, Postfach 3640, 7500 Karlsruhe 1, Federal Republic of Germany
113. C. D. Henning, Lawrence Livermore National Laboratory, P.O. Box 808, Livermore, CA 94550
114. G. K. Hess, Office of Fusion Energy, Department of Energy, Mail Stop ER-701, Washington, DC 20545
115. T. Hiraoka, JT-60 Project Office I, Japan Atomic Energy Research Institute, Tokai Research Establishment, Tokai, Ibaraki, Japan
116. R. L. Hirsch, Manager, Synthetic Fuels Research, Exxon Research and Engineering Company, P.O. Box 4255, Baytown, TX 77520
117. J. J. Holmes, Westinghouse-Hanford Engineering Development Laboratory, P.O. Box 1970, Richland, WA 99352
118. W. G. Homeyer, GA Technologies, Inc., P.O. Box 81608, San Diego, CA 92138
119. J. C. Hosea, Princeton Plasma Physics Laboratory, P.O. Box 451, Princeton, NJ 08544
120. D. Hwang, Princeton Plasma Physics Laboratory, P.O. Box 451, Princeton, NJ 08544
121. G. J. Inukai, Department E231, McDonnell Douglas Astronautics Company, P.O. Box 516, St. Louis, MO 63166
122. D. L. Jassby, Princeton Plasma Physics Laboratory, P.O. Box 451, Princeton, NJ 08544
123. J. B. Joyce, Princeton, Plasma Physics Laboratory, P.O. Box 451, Princeton, NJ 08544
124. R. A. Krakowski, CTR-12, Mail Stop 641, Los Alamos National Laboratory, P.O. Box 1663, Los Alamos, NM 87545
125. G. L. Kulcinski, University of Wisconsin, Department of Nuclear Engineering, Engineering Research Building, Room 439, 1500 Johnson Drive, Madison, WI 53706
126. D. L. Kummer, McDonnell Douglas Astronautics Company, P.O. Box 516, St. Louis, MO 63166
127. T. S. Latham, Mail Stop 44, United Technologies Research Center, Silver Lane, East Hartford, CT 06108
128. L. R. Ledman, Office of Fusion Energy, Department of Energy, Mail Stop G-256, Washington, DC 20545
129. L. M. Lidsky, MIT Plasma Fusion Center, 167 Albany Street, Cambridge, MA 02139

130. C. S. Liu, GA Technologies, Inc., P.O. Box 81608, San Diego, CA 92138
131. E. F. Lowell, General Manager, Energy Systems Programs Department Building 2-455, General Electric Company, 1 River Road, Schenectady, NY 12345
132. D. J. McFarlin, Mail Stop 44, United Technologies Research Center, Silver Lane, East Hartford, CT 06108
133. R. McGrath, Fusion Power Program, Argonne National Laboratory, 9700 South Cass Avenue, Argonne, IL 60439
134. V. A. Maroni, CEN/205, Argonne National Laboratory, 9700 South Cass Avenue, Argonne, IL 60439
135. W. Marton, Office of Fusion Energy, Office of Energy Research, Mail Station G-256, U.S. Department of Energy, Washington, DC 20545
136. L. G. Masson, EG&G Idaho, Idaho National Engineering Laboratory, P.O. Box 1625, Idaho Falls, ID 83401
137. D. G. McAlees, Exxon Nuclear Company, Inc., 777 106th Avenue, NE, Bellevue, WA 98009
138. D. M. Meade, Princeton Plasma Physics Laboratory, P.O. Box 451, Princeton, NJ 08544
139. A. T. Mense, Building 107, Post B2, McDonnell Douglas Astronautics Company, P.O. Box 516, St. Louis, MO 63166
140. L. Michaels, Princeton Plasma Physics Laboratory, P.O. Box 451, Princeton, NJ 08544
141. D. Mikkelsen, Princeton Plasma Physics Laboratory, P.O. Box 451, Princeton, NJ 08544
142. R. L. Miller, GA Technologies, Inc., P.O. Box 81608, San Diego, CA 92138
143. R. G. Mills, Princeton Plasma Physics Laboratory, P.O. Box 451, Princeton, NJ 08544
144. J. T. D. Mitchell, Culham Laboratory, Abingdon, Oxfordshire, OX14 3DB, United Kingdom
145. R. W. Moir, Lawrence Livermore National Laboratory, P.O. Box 808, Livermore, CA 94550
146. D. B. Montgomery, MIT Plasma Fusion Center, 167 Albany Street, Cambridge, MA 02139
147. K. Moses, R-1/1078, TRW Defense and Space Systems, 1 Space Park, Redondo Beach, CA 90278
148. R. E. Muller, Aerojet Manufacturing Company, P.O. Box 4210, Fullerton, CA 92934
149. A. E. Munier, Grumman Aerospace Company, P.O. Box 31, Bethpage, NY 11714
150. M. R. Murphy, Office of Fusion Energy, Department of Energy, Mail Station G-256, Washington, DC 20545
151. R. E. Nygren, FPP/207, Argonne National Laboratory, 9700 South Cass Avenue, Argonne, IL 60439
152. T. Ohkawa, GA Technologies, Inc., P.O. Box 81608, San Diego, CA 92138
153. M. Okabayashi, Princeton Plasma Physics Laboratory, P.O. Box 451, Princeton, NJ 08544
154. D. Overskei, GA Technologies, Inc., P.O. Box 81608, San Diego, CA 92138

155. R. R. Parker, Francis Bitter National Magnet Laboratory, 170 Albany Street, Cambridge, MA 02139
156. B. Pease, Culham Laboratory, Abingdon, Oxfordshire OX14 3DB, United Kingdom
157. M. Pelovitz, Princeton Plasma Physics Laboratory, P.O. Box 451, Princeton, NJ 08544
158. F. W. Perkins, Princeton Plasma Physics Laboratory, P.O. Box 451, Princeton, NJ 08544
159. M. Petravic, Princeton Plasma Physics Laboratory, P.O. Box 451, Princeton, NJ 08544
160. M. Porkolab, Massachusetts Institute of Technology, 77 Massachusetts Avenue, Cambridge, MA 02139
161. D. E. Post, Princeton Plasma Physics Laboratory, P.O. Box 451, Princeton, NJ 08544
162. L. K. Price, Department of Energy, Oak Ridge Operations, P.O. Box E, Oak Ridge, TN 37830
163. R. E. Price, Office of Fusion Energy, Office of Energy Research, Mail Station G-256, Department of Energy, Washington, DC 20545
164. D. H. Priester, Office of Fusion Energy, Office of Energy Research, Mail Station G-256, Department of Energy, Washington, DC 20545
165. F. A. Puhn, GA Technologies, Inc., P.O. Box 81608, San Diego, CA 92138
166. J. Purcell, GA Technologies, Inc., P.O. Box 81608, San Diego, CA 92138
167. R. V. Pyle, University of California, Lawrence Berkeley Laboratory, Berkeley, CA 94720
168. J. M. Rawls, GA Technologies, Inc., P.O. Box 81608, San Diego, CA 92138
169. P. J. Reardon, Princeton Plasma Physics Laboratory, P.O. Box 451, Princeton, NJ 08544
170. M. Roberts, Office of Fusion Energy, Department of Energy, Mail Stop G-256, Washington, DC 20545
171. J. D. Rogers, Los Alamos National Laboratory, P.O. Box 1663, Los Alamos, NM 87545
172. F. L. Robinson, Tennessee Valley Authority, 1300 Commerce Bank Building, Chattanooga, TN 37401
173. M. L. Rogers, Monsanto Research Corporation, Mound Laboratory Facility, P.O. Box 32, Miamisburg, OH 45342
174. M. N. Rosenbluth, RLM 11.218, Institute for Fusion Studies, University of Texas, Austin, TX 78712
175. L. Ruby, Lawrence Berkeley Laboratory, University of California, Berkeley, CA 94720
176. P. H. Rutherford, Princeton Plasma Physics Laboratory, P.O. Box 451, Princeton, NJ 08544
177. D. D. Ryutov, Institute of Nuclear Physics, Siberian Branch of the Academy of Sciences of the U.S.S.R., Sovetskaya St. 5, 630090 Novosibirsk, U.S.S.R.
178. M. M. Sabado, EBASCO Services, Inc., A Site, Building 1-A, Forrestal Campus, Princeton, NJ 08544
179. J. A. Schmidt, Princeton Plasma Physics Laboratory, P.O. Box 451, Princeton, NJ 08544

180. J. Schultz, MIT Plasma Fusion Center, 167 Albany Street, Cambridge, MA 02139
181. F. R. Scott, Electric Power Research Institute, P.O. Box 10412, Palo Alto, CA 94304
182. G. Sheffield, Princeton Plasma Physics Laboratory, P.O. Box 451, Princeton, NJ 08544
183. C. E. Singer, Princeton Plasma Physics Laboratory, P.O. Box 451, Princeton, NJ 08544
184. T. J. M. Sluyters, Accelerator Department, Brookhaven National Laboratory, Upton, NY 11973
185. D. Smith, Materials Science Division, Argonne National Laboratory, 9700 South Cass Avenue, Argonne, IL 60439
186. G. E. Smith, Grumman Aerospace Corporation, P.O. Box 31, Bethpage, NY 11714
187. R. I. Smith, Board Chairman, Public Service Electric and Gas Company, 80 Park Place, Newark, NJ 07101
188. L. Soroka, Lawrence Berkeley Laboratory, University of California, Berkeley, CA 94720
189. L. Southworth, GA Technologies, Inc., P.O. Box 81608, San Diego, CA 92138
190. I. Spigel, Lebedev Physical Institute, Leninsky Prospect 53, 117924 Moscow, U.S.S.R.
191. W. M. Stacey, Jr., Georgia Institute of Technology, School of Nuclear Engineering, Atlanta, GA 30332
192. D. Steiner, Rensselaer Polytechnic Institute, Nuclear Engineering Department, NES Building, Tibbits Avenue, Troy, NY 12181
193. E. Stern, Grumman Aerospace Corporation, CN-59, Forrestal Campus, Princeton, NJ 08544
194. L. D. Stewart, Princeton Plasma Physics Laboratory, P.O. Box 451, Princeton, NJ 08544
195. W. Stodiek, Princeton Plasma Physics Laboratory, P.O. Box 451, Princeton, NJ 08544
196. P. M. Stone, Office of Fusion Energy, Office of Energy Research, Mail Station G-256, Department of Energy, Washington, DC 20545
197. I. N. Sviatoslavsky, Room 33, Engineering Research Building, 1500 Johnson Drive, University of Wisconsin, Madison, WI 53706
198. T. Tamano, GA Technologies, Inc., P.O. Box 81608, San Diego, CA 92138
199. R. E. Tatro, Manager, Energy Systems, M.Z. 16-1070, General Dynamics-Convair Division, P.O. Box 80847, San Diego, CA 92138
200. F. Tenney, Princeton Plasma Physics Laboratory, P.O. Box 451, Princeton, NJ 08544
201. F. Thomas, B-20-5, Grumman Aerospace Corporation, Bethpage, NY 11714
202. K. I. Thomassen, Lawrence Livermore National Laboratory, P.O. Box 808, Livermore, CA 94550
203. R. J. Thome, Francis Bitter National Magnet Laboratory, 170 Albany Street, Cambridge, MA 02139
204. S. L. Thomson, Bechtel Group, Inc., P.O. Box 3965, San Francisco, CA 94119

205. V. T. Tolok, Kharkov Physical-Technical Institute, Academical St. 1, 310108 Kharkov, U.S.S.R.
206. C. Trachsel, McDonnell Douglas Astronautics Company, P.O. Box 516, St. Louis, MO 63166
207. J. R. Treglio, General Dynamics-Convair Division, P.O. Box 80847, San Diego, CA 92138
208. A. W. Trivelpiece, Office of Fusion Energy, Office of Energy Research, Mail Station G-256, Department of Energy, Washington, DC 20545
209. L. R. Turner, Fusion Power Program, Argonne National Laboratory, 9700 South Cass Avenue, Argonne, IL 60439
210. M. A. Ulrickson, Princeton Plasma Physics Laboratory, P.O. Box 451, Princeton, NJ 08544
211. E. H. Valeo, Princeton Plasma Physics Laboratory, P.O. Box 451, Princeton, NJ 08544
212. T. C. Varljen, Westinghouse Electric Corporation, P.O. Box 10864, Pittsburgh, PA 15236
213. R. Varma, Physical Research Laboratory, Navrangpura, Ahmedabad, India
214. H. F. Vogel, Los Alamos National Laboratory, P.O. Box 1663, Los Alamos, NM 87545
215. A. Wait, Building 36-421, General Electric Company, 1 River Road, Schenectady, NY 12345
216. K. E. Wakefield, Princeton Plasma Physics Laboratory, P.O. Box 451, Princeton, NJ 08544
217. D. Weldon, Los Alamos National Laboratory, P.O. Box 1663, Los Alamos, NM 87545
218. J. C. Wesley, GA Technologies, Inc., P.O. Box 81608, San Diego, CA 92138
219. S. Whitley, Tennessee Valley Authority, 1300 Commerce Bank Building, Chattanooga, TN 37401
220. W. R. Wilkes, Monsanto Research Corporation, Mound Laboratory Facility, P.O. Box 32, Miamisburg, OH 45342
221. J. E. Wilkins, EG&G Idaho, Idaho National Engineering Laboratory, P.O. Box 1625, Idaho Falls, ID 83401
222. H. Willenberg, Mathematical Sciences Northwest, Inc., P.O. Box 1887, Bellevue, WA 98009
223. J. E. C. Williams, Francis Bitter National Magnet Laboratory, 170 Albany Street, Cambridge, MA 02139
224. P. Willis, Building 23, Room 298, General Electric Company, 1 River Road, Schenectady, NY 12345
225. T. F. Yang, MIT Plasma Fusion Center, 167 Albany Street, Cambridge, MA 02139
226. H. H. Yoshikawa, W/A-62, Hanford Engineering Development Laboratory, P.O. Box 1970, Richland, WA 99352
227. K. M. Young, Princeton Plasma Physics Laboratory, P.O. Box 451, Princeton, NJ 08544
228. N. E. Young, EBASCO Services, Inc., Princeton Plasma Physics Laboratory, P.O. Box 451, Princeton, NJ 08544
229. K. M. Zwilsky, National Materials Advisory Board, National Academy of Sciences, 2101 Constitution Avenue NW, Washington, DC 20418

230. Bibliothek, Max-Planck Institut fur Plasmaphysik, D-8046 Garching bei Munchen, Federal Republic of Germany
231. Bibliothek, Institut fur Plasmaphysik, KFA, Postfach 1913, D-5170 Julich, Federal Republic of Germany
232. Bibliotheque, Centre de Recherches en Physique des Plasmas, 21 Avenue des Bains, 1007 Lausanne, Switzerland
233. Bibliotheque, Service du Confinement des Plasmas, CEA, B.P. No. 6, 92 Fontenay-aux-Roses (Seine), France
234. Documentation S.I.G.N., Departement de la Physique du Plasma et de la Fusion Controlee, Association EURATOM-CEA, Centre d'Etudes Nucleaires, B.P. 85, Centre du Tri, 38041 Grenoble, Cedex. France
235. Library, Culham Laboratory, UKAEA, Abingdon, Oxfordshire OX14 3DB, England
236. Library, FOM Instituut voor Plasma-Fysica, Rijnhuizen, Jutphaas, Netherlands
237. Library, Institute of Physics, Academia Sinica, Beijing, Peoples Republic of China
238. Library, Institute for Plasma Physics, Nagoya University, Nagoya 464, Japan
239. Library, International Centre for Theoretical Physics, Trieste, Italy
240. Library, JET Joint Undertaking, Abingdon, Oxfordshire, OX14, 3DB England
241. Library, Laboratoria Gas Ionizzati, Frascati, Italy
242. Plasma Research Laboratory, Australian National University, P.O. Box 4, Canberra, ACT 2000, Australia
243. Thermonuclear Library, Japan Atomic Energy Research Institute, Tokai, Naka, Ibaraki, Japan
244. Library, Plasma Physics Laboratory, Kyoto University, Gokasho Uji, Kyoto, Japan
245. Office of the Assistant Manager for Energy Research and Development, Department of Energy, Oak Ridge Operations, Oak Ridge, TN 37830

246-449. Given distribution as shown in TID-4500, Magnetic Fusion Energy, (Distribution Category UC-20 c,d: Reactor Materials and Fusion Systems)

ABSTRACT

The Toroidal Fusion Core Experiment (TFCX) is proposed to be an ignition device with a low safety factor ($q \sim 2.0$), rf or rf-assisted startup, long inductive burn pulse ($\sim$300 s), and an elongated plasma cross section ($\kappa = 1.6$) with moderate triangularity ($\delta = 0.3$). System trade studies have been carried out to assist in choosing an appropriate candidate for TFCX conceptual design. This report describes an important element in these system studies — the magnetohydrodynamic (MHD) equilibrium modeling of the TFCX poloidal field (PF) coil system and its impact on the choice of machine size. Reference design points for the all-superconducting toroidal field (TF) coil (TFCX-S) and hybrid (TFCX-H) options are presented that satisfy given PF system criteria, including volt-second requirements during burn, mechanical configuration constraints, maximum field constraints at the superconducting PF coils, and plasma shape parameters. Poloidal coil current waveforms for the TFCX-S and TFCX-H reference designs consistent with the equilibrium requirements of the plasma startup, heating, and burn phases of a typical discharge scenario are calculated. Finally, a possible option for quasi-steady-state operation is discussed.

DOE Form RA-426
(10/80)

U.S. DEPARTMENT OF ENERGY

OMB NO. 038-R0190

DOE AND MAJOR CONTRACTOR RECOMMENDATIONS FOR ANNOUNCEMENT AND DISTRIBUTION OF DOCUMENTS

See Instructions on Reverse Side

1. DOE Report No.	2. Contract No.	3. Subject Category No.
ORNL/FEDC-83/10	W-7405-eng-26	UC-20c,d

4. Title
Equilibrium Modeling of the TFCX Poloidal Field Coil Systems

5. Type of Document ("x" one)
- [X] a. Scientific and technical report
- [ ] b. Conference paper: Title of conference _____
  Date of conference _____
  Exact location of conference _____ Sponsoring organization _____
- [ ] c. Other (specify planning, educational, impact, market, social, economic, thesis, translations, journal article manuscript, etc.)

6. Copies Transmitted ("x" one or more)
- [X] a. Copies being transmitted for standard distribution by DOE TIC
- [ ] b. Copies being transmitted for special distribution per attached complete address list.
- [ ] c. Two completely legible, reproducible copies being transmitted to DOE–TIC. (Classified documents see instructions)
- [ ] d. Twenty-seven copies being transmitted to DOE–TIC for TIC processing and NTIS sales.

7. Recommended Distribution ("x" one)
- [X] a. Normal handling (after patent clearance): no restraints on distribution except as may be required by the security classification.

Make available only [ ] b. To U.S. Government agencies and their contractors. [ ] c. within DOE and to DOE contractors. [ ] d. within DOE. [ ] e. to those listed in item 13 below.

- [ ] f. Other (Specify)

8. Recommended Announcement ("x" one)
- [X] a. Normal procedure may be followed. [ ] b. Recommend the following announcement limitations:

9. Reason for Restrictions Recommended in 7 or 8 above.
- [ ] a. Preliminary information. [ ] b. Prepared primarily for internal use. [ ] c. Other (Explain)

10. Patent, Copyright and Proprietary Information

Does this information product disclose any new equipment, process or material? [ ] No [ ] Yes If so, identify page nos. _____

Has an invention disclosure been submitted to DOE covering any aspect of this information product? [ ] No [ ] Yes
If so, identify the DOE (or other) disclosure number and to whom the disclosure was submitted.

Are there any patent-related objections to the release of this information product? [ ] No [ ] Yes If so, state these objections.

Does this information product contain copyrighted material? [ ] No [ ] Yes

If so, identify the page number _____ and attach the license or other authority for the government to reproduce.

Does this information product contain proprietary information? [ ] No [ ] Yes If so, identify the page numbers _____.

("x" one [X] a. DOE patent clearance has been granted by responsible DOE patent group.
[ ] b. Document has been sent to responsible DOE patent group for clearance.

11. National Security Information (For classified document only; "x" one)
Document [ ] a. does [ ] b. does not contain national security information

12. Copy Reproduction and Distribution
Total number of copies reproduced 449 Number of copies distributed outside originating organization 405

13. Additional Information or Remarks (Continue on separate sheet, if necessary)

14. Submitted by (Name and Position) (Please print or type)
Nancy V. Taylor, Supervisor, Laboratory Records Dept.

Organization
Oak Ridge National Laboratory

Signature Nancy V. Taylor Date March 26, 1984

INSTRUCTIONS

Who uses this form: All DOE and DOE contractors except those contractors and grantees specifically instructed by their DOE contract administrator to use the shorter Form RA-427.

When to use: Submit one copy of this form with each document that is sent to the DOE Technical Information Center (TIC) in accordance with the requirements of DOE Order 1340.1.

Where to send: Forward this form and the document(s) to:

USDOE-TIC
P.O. Box 62
Oak Ridge, TN 37830

Item instructions:

Item 1. The DOE report number will be constructed as follows:
(a) Major DOE Laboratories and contractors that have been assigned TIC-approved codes will use their approved system, e.g., BNL, BMI, PNL. Sequential numbers will be assigned to each report by the originating laboratory or contractor.
(b) Contractors that do not have TIC-approved identifying codes will create their unique numbers by (1) identifying the report with code DOE, (2) selecting the basic seven characters (two alphabetic and five numeric) for the applicable contract number, and (3) adding sequential numbers for each report generated under the contract. Slash marks and hyphens should be applied as shown in the examples below.

Reports issued in more than one binding or reissued as revisions or later editions will be identified by adding the additional suffixes to the basic number, e.g., Rev., Revision; Vol., Volume; Pt., Part; Add., Addendum; Ed., Edition.

Examples:

Major laboratories and contractors with approved codes
BNL-1874

Contractors without approved codes
For Contract DE-AC01-78RA01834.M002
DOE/RA/01834-1
DOE/RA/01834-2
DOE/RA/01834-2 Rev. 1
(The modification number, if any, normally shown as .M002, etc., following the basic five-digit number, is not used in the report number.)

Item 2. Self-explanatory.

Item 3. Insert the appropriate subject category from DOE/TIC-4500 ("Standard Distribution for Unclassified Scientific and Technical Reports") or M-3679 ("Standard Distribution for Classified Scientific and Technical Reports") for both classified and unclassified documents, whether or not printed for standard distribution.

Item 4. Give title exactly as on the document itself unless title is classified. In that case, omit title and state "classified title" in the space for item 4.

Item 5. Self explanatory.

Item 6. *a.* If box *a* is checked, the number of copies specified for the appropriate category or categories in M-3679 or DOE/TIC-4500 will be forwarded to TIC for distribution.

b. If box *b* is checked, a complete address list must be provided TIC.

c. If box *c* is checked, at least one copy will be original ribbon or offset and be completely legible. A clear carbon copy is acceptable as a second reproducible copy. Classified documents, send one copy except where special distribution requires more copies.

d. If box *d* is checked, 27 copies will be forwarded to TIC, 2 will be retained for processing and 25 will be sent to NTIS for public availability.

Item 7. If box *a* is checked for an unclassified document, it may be distributed by TIC (after patent clearance) to addressees listed in DOE/TIC-4500 for the appropriate subject category, to libraries in the U.S. and abroad which through purchase of microfiche maintain collections of DOE reports, and to the National Technical Information Service for sale to the public.

If box *a* is checked for a classified document, it may be distributed by TIC to addressees listed in M-3679 for the appropriate subject category.

If a box other than *a* is checked, the recommended limitation will be followed unless TIC receives other instructions from the responsible DOE program division.

Box *f* may be checked in order to specify special instructions, such as "Make available only as specifically approved by the program division."

Item 8. *a.* Announcement procedures are normally determined by the distribution that is to be given a document. If box *a* in item 7 is checked for an unclassified document, it will normally be listed in the weekly "Accessions of Unlimited Distribution Reports by TIC" (DOE/TIC-4401) and may be abstracted in *Energy Research Abstracts (ERA).*

A classified document, or an unclassified document for which box *b, c, d, e,* or *f* in item 7 is checked, may be cited with appropriate subject index terms in *Abstracts of Limited Distribution Reports (ALDR).*

b. If the normal announcement procedures described in 8*a* are not appropriate, check 8*b* and indicate recommended announcement limitations.

Item 9. Self-explanatory.

Item 10. It is assumed that there is no objection to publication from the standpoint of the originating organization's patent interest. Otherwise explain in item 13.

Item 11. If box *a* is checked, the document cannot be made available to Access Permit holders (Code of Federal Regulation 10 CFR, Part 26, subpart 26.6), if box *b* is checked, TIC will determine whether or not to make it available to them.

Item 12. Self-explanatory.

Item 13. Self-explanatory.

Item 14. Enter name of person to whom inquiries concerning the recommendations on this form may be addressed.